NJC
New Journal of Chemistry
A journal for new directions in chemistry

Accepted Manuscript

This article can be cited before page numbers have been issued, to do this please use: A. T. Hand, A. A. Fakolujo, J. Krzystek, M. Ozerov, L. L. Daemen, J. Xing, Z. Gai, R. Jin, J. Telser, A. A. Podlesnyak and Z. Xue, *New J. Chem.*, 2025, DOI: 10.1039/D5NJ01857A.

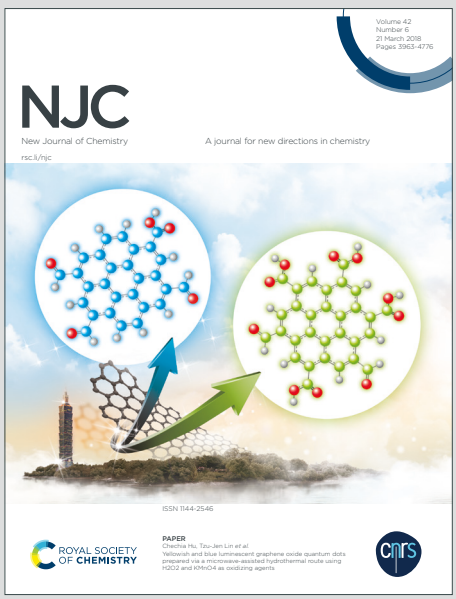

This is an Accepted Manuscript, which has been through the Royal Society of Chemistry peer review process and has been accepted for publication.

Accepted Manuscripts are published online shortly after acceptance, before technical editing, formatting and proof reading. Using this free service, authors can make their results available to the community, in citable form, before we publish the edited article. We will replace this Accepted Manuscript with the edited and formatted Advance Article as soon as it is available.

You can find more information about Accepted Manuscripts in the Information for Authors.

Please note that technical editing may introduce minor changes to the text and/or graphics, which may alter content. The journal's standard Terms & Conditions and the Ethical guidelines still apply. In no event shall the Royal Society of Chemistry be held responsible for any errors or omissions in this Accepted Manuscript or any consequences arising from the use of any information it contains.

View Article Online
DOI: 10.1039/D5NJ01857A

Advanced spectroscopic studies of $(PPh_4)_2[Co(N_3)_4]$, a field-induced single-ion magnet

Adam T. Hand,[a] Adiat A. Fakolujo,[a] J. Krzystek,[b] Mykhaylo Ozerov,[b] Luke L. Daemen,[c] Jie Xing,[d] Zheng Gai,[e] Rongying Jin,[d] Joshua Telser,[f] Andrey A. Podlesnyak,[c] and Zi-Ling Xue[a,*]

[a] *Department of Chemistry, University of Tennessee, Knoxville, Tennessee 37996, USA*

[b] *National High Magnetic Field Laboratory, Florida State University, Tallahassee, Florida 32310, USA*

[c] *Neutron Scattering Division, Oak Ridge National Laboratory, Oak Ridge, Tennessee 37831, USA*

[d] *SmartState Center for Experimental Nanoscale Physics, Department of Physics and Astronomy, University of South Carolina, Columbia, SC 29208, USA*

[e] *Center for Nanophase Materials Sciences, Oak Ridge National Laboratory, Oak Ridge, Tennessee 37831, USA*

[f] *Department of Biological, Physical and Health Sciences, Roosevelt University, Chicago, IL 60605, USA*

Abstract

High-spin Co^{II} complex $(PPh_4)_2[Co(N_3)_4]$ (**Co-N$_3$**) has been investigated using advanced spectroscopic techniques [far-IR magneto-spectroscopy (FIRMS), high-frequency and -field EPR (HFEPR), and inelastic neutron scattering (INS)] to study its zero-field-splitting (ZFS), giving spin-Hamiltonian (SH) parameters. The analysis of multi-frequency HFEPR reveals the easy-axis anisotropy with a D value of –10.39(5) cm^{-1} and rhombic ratio (E/D) of 0.21(1). The magnetic properties have also been probed by direct-current (DC) magnetometry, suggesting minor differences in anisotropy from the previously reported polymorph (**Co-N$_3$'**). Ligand-field theory (LFT) analysis indicates the structures of **Co-N$_3$** and **Co-N$_3$'** are closer to D_{2d} symmetry than other symmetries considered. Alternate-current (AC) susceptibility reveals slow magnetic relaxation under an applied field, indicating **Co-N$_3$** is a field-induced single-ion magnet (SIM). While both **Co-N$_3$** and **Co-N$_3$'** were studied by DC magnetometry, one unusual aspect of the current work on **Co-N$_3$** is that advanced spectroscopies HFEPR, FIRMS, and INS were used to directly observe transitions between ZFS split states, giving accurate SH parameters.

View Article Online
DOI: 10.1039/D5NJ01857A

Introduction

Single-ion magnets (SIMs) are a fascinating class of molecular materials that exhibit magnetic behavior typically associated with bulk magnets, but on a molecular scale. These materials ideally can retain the magnetization without an external magnetic field. This makes them highly valuable for potential applications in high-density data storage, quantum computing, and molecular spintronics.[1-21] The ability of SIMs to operate as molecular magnets arises from their large magnetic anisotropy and slow relaxation of the magnetization.

Transition metal complexes have been of intense interest, in part as their magnetic anisotropy is much more tunable than lanthanide complexes. This is because the ligand field effects in the former are more easily tuned than the spin-orbit coupling (SOC) in the latter.[6, 14, 17, 22-25] The Co^{II}-based SIMs are the most explored with various coordination environments and geometries.[26] Four-coordinate tetrahedral Co^{II}-based SIMs are of particular interest.[27-52] Among these are homoleptic SIMs with CoX_4 units (X = O, S, Se and Te;[34-43] N;[44-51, 53, 54] Cl[55, 56]) have been reported. When the coordination environment is less than cubic (in this present case, T_d), the magnetic properties are dominated by the extent of deviation from T_d symmetry.[57-59,60] Slight distortions of the crystal field environment can lead to significant zero-field splitting (ZFS) and slow relaxation of the magnetization. Thus, understanding and controlling these deviations are crucial for optimizing the magnetic properties of Co^{II}-based SIMs, as these subtle changes can significantly influence the overall magnetic behavior and potential applications of these materials.

Tetrahedral tetrakis(pseudohalido) Co^{2+} complexes, containing the anions $[Co(N_3)_4]^{2-}$,[54, 61, 62] $[Co(NCO)_4]^{2-}$,[51, 54] and $[Co(NCS)_4]^{2-}$,[48-51, 54] have been studied to probe how deviations from T_d affect their properties including ZFS. Chen and coworkers recently gave a detailed summary of such complexes.[54] Tetraazide Co^{2+} complexes include $(PPh_4)_2[Co(N_3)_4]$ with two polymers, **Co-N$_3$**[61] and **Co-N$_3$′**,[54] and $[Co(bdmpzpy)_2][Co(N_3)_4]$ (bdmpzpy = 2,6-bis[(3,5-dimethyl-pyrazol-1H-yl)-methyl]pyridine) studied by Massoud and coworkers.[62] Sen and Mondal reported the synthesis and crystal structure of **Co-N$_3$**, the first polymorph of $(PPh_4)_2[Co(N_3)_4]$ (structure in Fig. 1a).[61] Chen and coworkers later reported the formation and crystal structure of **Co-N$_3$'**, the second polymorph, as well as its magnetic properties by DC and AC magnetometry and HFEPR.[54] To our knowledge, the magnetic properties of the first polymorph **Co-N$_3$** and comparison of two polymorphs have not been reported.

View Article Online
DOI: 10.1039/D5NJ01857A

SHAPE analysis of $(PPh_4)_2[Co(N_3)_4]$ (**Co-N$_3$**) below shows that the complex could be described by the distorted D_{2d} symmetry. D and E are axial and rhombic ZFS parameters, respectively. As shown in Fig. 1b, the magnitude of ZFS, $2D' = 2(D^2 + 3E^2)^{1/2}$, reflects the deviation from the T_d symmetry. The spin Hamiltonian for an $S = 3/2$ complex with an applied magnetic field $\boldsymbol{B}$ is given in Eq. 1:

$$\hat{H}_S = D\left(\hat{S}_z^2 - \frac{5}{4}\right) + E\left(\hat{S}_x^2 - \hat{S}_y^2\right) + \mu_B g_x B_x \hat{S}_x + \mu_B g_y B_y \hat{S}_y + \mu_B g_z B_z \hat{S}_z \quad (1)$$

where $\hat{S}$ is the spin operator, μ_B is the electron Bohr magneton, $g_{x,y,z}$ are the g-factor components, and $\boldsymbol{B} = (B_x, B_y, B_z)$ is the applied magnetic field vector. For non-zero rhombicity $E \neq 0$, mixing of the M_S magnetic sublevels occurs as shown in Fig. 1, allowing for quantum tunneling. This mixing is a function of rhombicity ratio (E/D) by $\tan(2\beta) = \sqrt{3}(E/D)$, where β is the mixing angle. Mixing coefficients, $a = \cos\beta$ and $b = \sin\beta$, are therefore used to weight ZFS states by rhombicity.[63, 64]

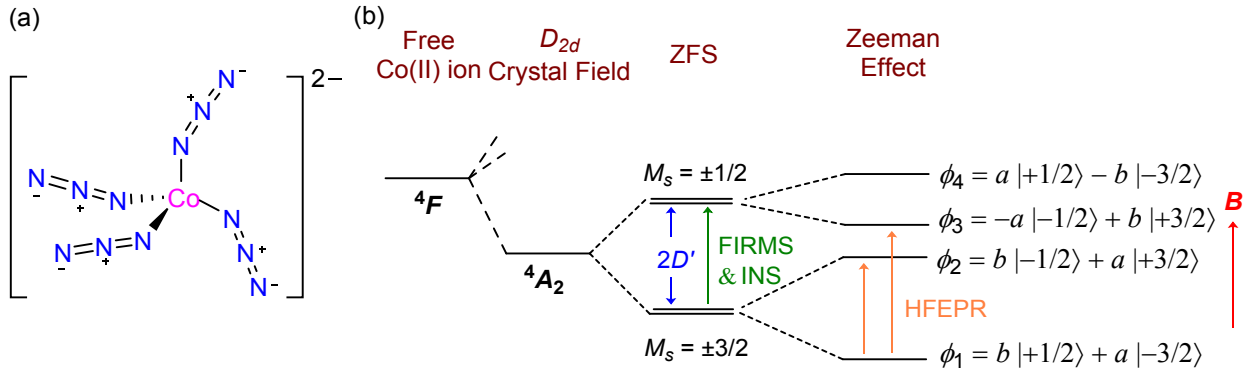

Fig. 1. (a) Structure of the $[Co(N_3)_4]^{2-}$ anion in **Co-N$_3$**. (b) Splitting diagram for **Co-N$_3$** with dominant easy-axis anisotropy ($D < 0$) with symmetry lower (i.e., $x \neq y$, $E \neq 0$) than D_{2d}. $^4A_2$ is the electronic ground state based on descending the symmetry from the $^4T_{1g}$ electronic ground state of a high-spin d^7 O_h complex to D_{2d}.[65] In other words, the quartet levels in $^4A_2$ undergo zero-field splitting (ZFS) into two doublets split by $2D' = 2(D^2 + 3E^2)^{1/2}$. When $x \neq y$ ($E \neq 0$), mixing of M_S magnetic sublevels occurs, where the mixing coefficients $a = \cos\beta$ and $b = \sin\beta$ are described by the mixing angle β that depends on the rhombicity as $\tan 2\beta = \sqrt{3}\ (E/D)$.[60] The mixing allows for quantum tunneling.[63, 64] Spectroscopies used in the current work are shown

View Article Online
DOI: 10.1039/D5NJ01857A

here, including far-IR magneto-spectroscopy (FIRMS),[44, 66-81] high-frequency and -field EPR (HFEPR),[19, 20, 77, 82-92] and inelastic neutron scattering (INS).[3, 93-108]

Herein, we provide magnetic and spectroscopic studies of $(PPh_4)_2[Co(N_3)_4]$ (**Co-N$_3$**), which adopts a distorted tetrahedral geometry. To our knowledge, the structure has two polymorphs (**Co-N$_3$** and **Co-N$_3$'**). The magnetic properties of the second polymorph **Co-N$_3$'** were probed recently.[54] Our goals in this work are: (1) Characterize the first polymorph **Co-N$_3$** by advanced spectroscopies (FIRMS, HFEPR, and INS); (2) Study the polymorph by DC and AC magnetometry, comparing the spin-Hamiltonian parameters between the advanced spectroscopies and magnetometry; (3) Determine if the first polymorph **Co-N$_3$** has the single-ion magnet (SIM) properties; (4) Compare the results of both polymorphs with the assistance of the *SHAPE* analysis and ligand-field theory (LFT) calculations. We are also interested in whether there is a correlation between the degree of deviation from the perfect T_d symmetry and zero-field splitting (ZFS) of the magnetic levels in Fig. 1. While DC and AC magnetometry has been widely used in the studies of SIMs, the current work is unusual in that advanced spectroscopies, HFEPR, FIRMS, and INS, have been used to probe magnetic properties of **Co-N$_3$**, in addition to DC magnetometry.

Results and discussion

Determination of the zero-field splitting (ZFS) by FIRMS, HFEPR, and INS

The separation between Kramers doublets $M_S = |\pm 3/2\rangle$ and $|\pm 1/2\rangle$ is $2D'$ for an $S = 3/2$ ion such as Co^{II}. For **Co-N$_3$** here, the transition between these levels has been directly determined by FIRMS,[44, 66-81] HFEPR,[19, 20, 77, 82-92] and INS.[3, 93-108] FIRMS and INS allows the direct observation of ZFS, whereas multiple-frequency HFEPR has determined the spin-Hamiltonian parameters, D, E, and g, including the negative sign of D, suggesting the easy-axis anisotropy in **Co-N$_3$**. It should be pointed that HFEPR spectra of **Co-N$_3$'** did not show a signal, as reported in Ref. 54. Results of the current work are summarized in Table 1 below. Basic features of HFEPR, FIRMS, and INS are presented in earlier publications, including their reviews in Ref. 109, Ref. 110, and Table 4 in Ref. 68. INS is also reviewed in Ref. 108.

View Article Online
DOI: 10.1039/D5NJ01857A

FIRMS

Far-infrared magneto-spectroscopy (FIRMS) refers to Fourier-transform FIR (in the range 12-720 cm-1) in the presence of an applied magnetic field (0-17 T). This technique is useful for identifying the magnetic dipole-allowed transition, $M_S = |\pm 3/2\rangle \rightarrow |\pm 1/2\rangle$, in **Co-N$_3$** at 0 T.[110-112] As field increases, the Kramers doublets split into their respective M_S levels. In FIRMS, the Zeeman effect and different orientations of the powder samples lead to shifts of magnetic transitions. The FIRMS transmission spectrum at 5.5 K and at 0 and 17 T (Fig. 2-Top) shows magnetic field dependence within the selected energy range. Further analysis can be performed by constructing a heat map (Fig. 2-Bottom) of the normalized transmittance which shows a color gradient where the blue color represents a deviation from the average intensity across all magnetic fields caused by spectral features with the magnetic field dependence, while the yellow color corresponds to regions indifferent to magnetic field. Energy of the magnetic transition changes with field increase due to Zeeman effect (Fig. 1). In Fig. 2, the Zeeman effect could be observed, which can be traced back to its origin at 0 T at 22(1) cm^{-1}. Thus, this value is assigned to be the zero-field transition between Kramers doublets (ZFS, $2D'$).

The phonons **B**, **C**, and **D** show spin-phonon couplings. Phonons here refer to both intramolecular and intermolecular (or lattice) vibrations. For the 2-D FIRMS map in Fig. 2b, a simplified Hamiltonian for the coupling between the magnetic excited level $|\phi_j\rangle$ and *one* phonon excited state $|n\rangle$ is given by the following 2 × 2 matrix in Eq. 2:[113]

$$H = \begin{pmatrix} E_{\mathrm{sp}} & \Lambda \\ \Lambda & E_{\mathrm{ph}} \end{pmatrix} \qquad (2)$$

where E_{sp} and E_{ph} = expected energies of the magnetic and phonon excitations, respectively; Λ = spin-phonon coupling constant.

Solving the matrix gives two eigenvalues $E_{\pm}$ (with the associated avoided-crossing peaks $|\Psi_{\pm}\rangle$) in the secular Eq. 3.

$$\begin{vmatrix} E_{\mathrm{sp}} - E_{\pm} & \Lambda \\ \Lambda & E_{\mathrm{ph}} - E_{\pm} \end{vmatrix} = 0 \qquad (3)$$

View Article Online
DOI: 10.1039/D5NJ01857A

During the spin-phonon coupling, $|\Psi_+\rangle$ shifts to higher E_+, while $|\Psi_-\rangle$ shifts to lower E_- in the avoided crossing, as shown in Fig. 2c. Eqs. 2-3 give a model to understand spin-phonon coupling in the FIRMS map and calculate the coupling constants Λ.

This model can be expanded to a 4 × 4 matrix in Eq. 4 involving the couplings of the magnetic transition with all four phonons **B**, **C**, and **D** simultaneously. Here, interactions (couplings) among phonons are ignored. Thus, the off-diagonal elements between any two phonons are set to be 0. The ZFS peak (E_{sp}) was modeled every 0.5 T from 0 T to 17 T for the transmittance peak, giving the coupling constants Λ_1 = 0.5(5) cm^{-1}, Λ_2 = 1.0(5) cm^{-1}, and Λ_3 = 1.5(5) cm^{-1}. **B**, **C**, and **D** are phonons in the crystalline solid of **Co-N$_3$** observed to undergo spin-phonon couplings, even though there are likely additional IR-active phonons in the 22-50 cm^{-1} region. The spin-phonon couplings here are similar to other reported complexes.[60, 67, 68, 114]

$$H = \begin{pmatrix} E_{sp-\mathrm{A}} & \Lambda_1 & \Lambda_2 & \Lambda_3 \\ \Lambda_1 & E_{ph-\mathrm{B}} & 0 & 0 \\ \Lambda_2 & 0 & E_{ph-\mathrm{C}} & 0 \\ \Lambda_3 & 0 & 0 & E_{ph-\mathrm{D}} \end{pmatrix} \quad (4)$$

View Article Online
DOI: 10.1039/D5NJ01857A

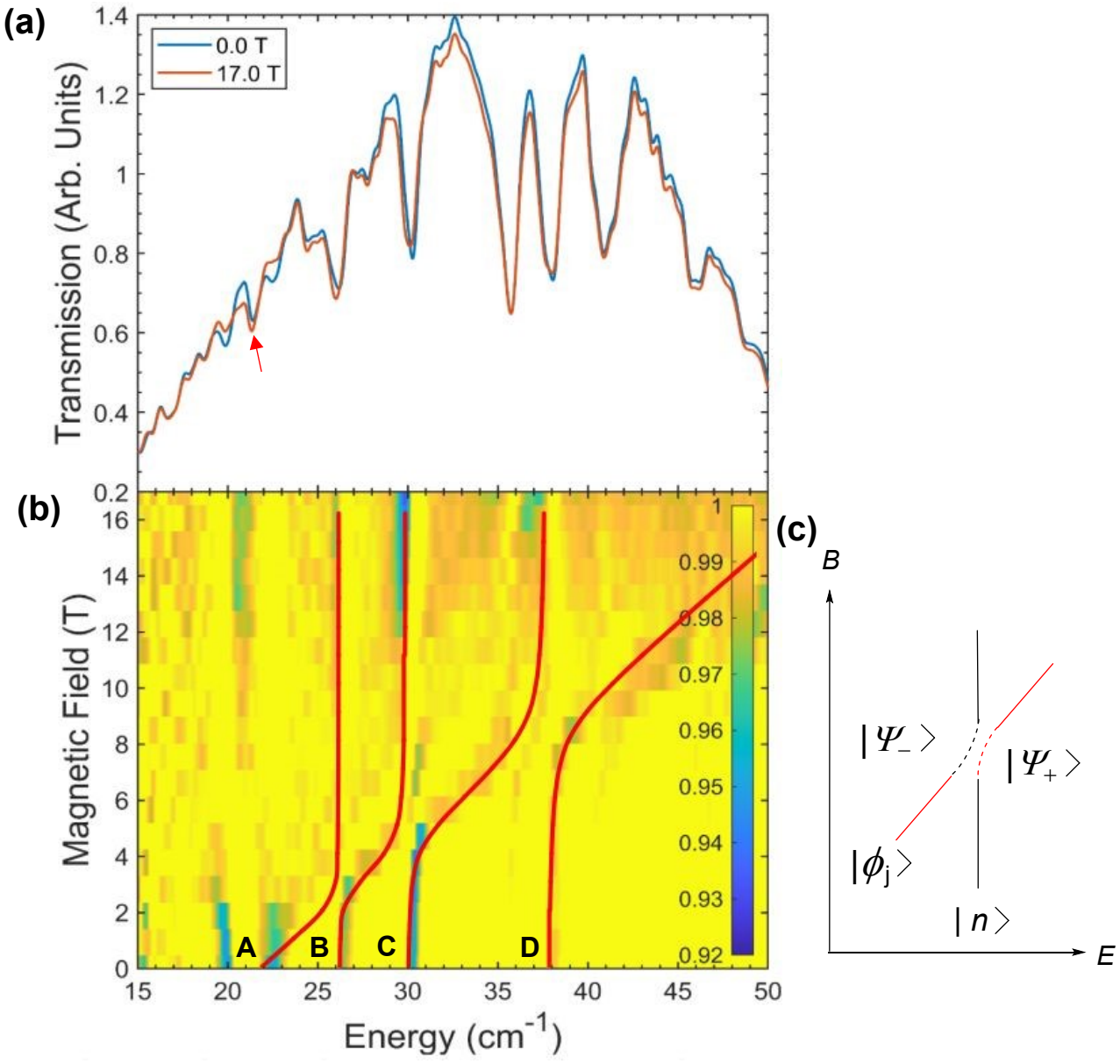

Fig. 2. (a) FIRMS transmission spectra of **Co-N_3** at 5.5 K for 0 and 17 T. (b) Heat map of the normalized transmittance where yellow regions are indifferent to magnetic field. The arrow points to the magnetic transition at 0 T. Fitting of the spin-phonon couplings in red lines by Eq. 4 gives coupling constants of the magnetic peak **A** with phonons **B**, **C**, and **D**: Λ_1 = 0.5(5), Λ_2 = 1.0(5), and Λ_3 = 1.5(5) cm^{-1}, respectively. (c) Schematic representation of an avoided crossing.[19, 67]

View Article Online
DOI: 10.1039/D5NJ01857A

HFEPR

HFEPR of **Co-N_3** yields well-defined spectra characteristic for an $S = 3/2$ spin state with negative D (Fig. 3, top trace). The two peaks visible in the spectrum taken at 4.5 K are attributed to the z- and x-turning points, respectively, of the $M_S = |{-3/2}\rangle \rightarrow |{+3/2}\rangle$ transition within the ground $M_S = \pm 3/2$ spin sublevel (implying that D is negative). The derivative spectral shape of the z turning point suggests that the crystallites undergo a torquing effect (reorientation) in the magnetic field.

The derivative spectral shape of the z-turning point suggests that the crystallites undergo a torquing effect (reorientation) in the magnetic field.[92] To prevent this phenomenon, the sample was pressed into a pellet together with *n*-eicosane which produced spectra distinctly different in shape compared to the sample "as is" (Fig. 3, middle trace). In particular, the resonance corresponding to the z-turning point became much weaker and absorptive, as expected, while the one corresponding to the x-turning point gained intensity and remained derivative. The resulting spectrum could be very satisfactorily simulated as a powder pattern originating from a random orientation of microcrystallites regarding the magnetic field (Fig. 3, bottom trace).

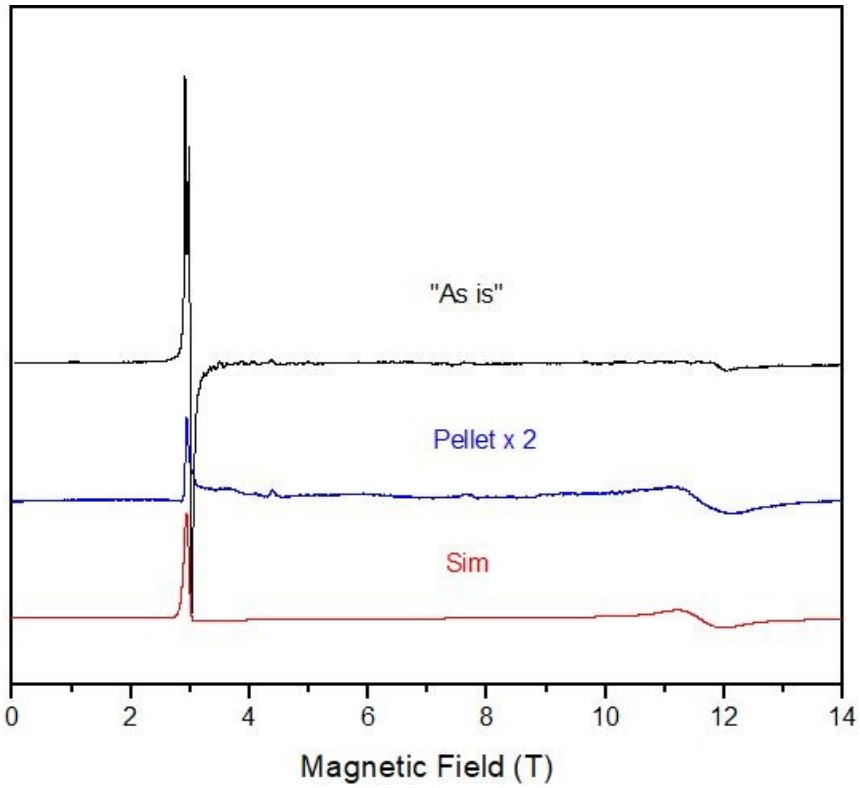

Fig. 3. HFEPR spectra of **Co-N_3** at 4.5 K and 276 GHz. Top trace (black): sample "as is".

View Article Online
DOI: 10.1039/D5NJ01857A

Middle trace (blue): sample constrained in a pellet with *n*-eicosane. Bottom trace (red): a simulation of the pellet spectrum using spin-Hamiltonian parameters $D = -10.39$ cm^{-1}, $|E| = 2.22$ cm^{-1}, $g = [2.21, 2.35, 2.35]$.

We offer two additional HFEPR spectra, one taken at a much lower frequency 71 GHz (Fig. S1), where it is possible to see all three turning points of the $M_S = |{-3/2}\rangle \rightarrow |{+3/2}\rangle$ transition: $B_0 \parallel x$ at 3.4 T, $B_0 \parallel y$ at 4.9 T, and $B_0 \parallel z$ at 0.75 T. At higher frequencies, the *y*-turning point moves rapidly beyond the magnet range, as shown in Fig. 4. The other spectrum, Fig. S2, shows a much higher frequency, 476.2 GHz, where it is possible to discern the inter-Kramers transition at 3.2 T between the $M_S = |{+3/2}\rangle$ and $|{-1/2}\rangle$ spin sublevels. Because of the mixing of the four M_S magnetic sublevels (Fig. 1), such a transition is partially allowed, despite being nominally $\Delta M_S = 2$. An observation of this transition is paramount in determining the ZFS parameters from HFEPR alone. The peak at 5.2 T is the *z*-turning point of the intra-Kramers $M_S = |{-3/2}\rangle \rightarrow |{+3/2}\rangle$ transition observed before at lower frequencies.

The final spin-Hamiltonian parameters were obtained *not* from single-frequency spectra but from the multi-frequency data set comprising of collected turning points at multiple frequencies, along the tunable-frequency EPR principle,[115] as shown in Fig. 4. These parameters are: $D = -10.39(5)$ cm^{-1}, $|E| = 2.22(7)$ cm^{-1} ($|E/D| = 0.21(1)$, $2D' = 22.1(1)$ cm^{-1}), $\boldsymbol{g} = [g_{xx}, g_{yy}, g_{zz}] = [2.21(4), 2.35(11), 2.35(2)]$. The FIRMS heat map is overlayed in Fig. 4 showing a good agreement with HFEPR. The HFEPR and FIRMS analyses are independent of each other in obtaining the $2D'$ value.

View Article Online
DOI: 10.1039/D5NJ01857A

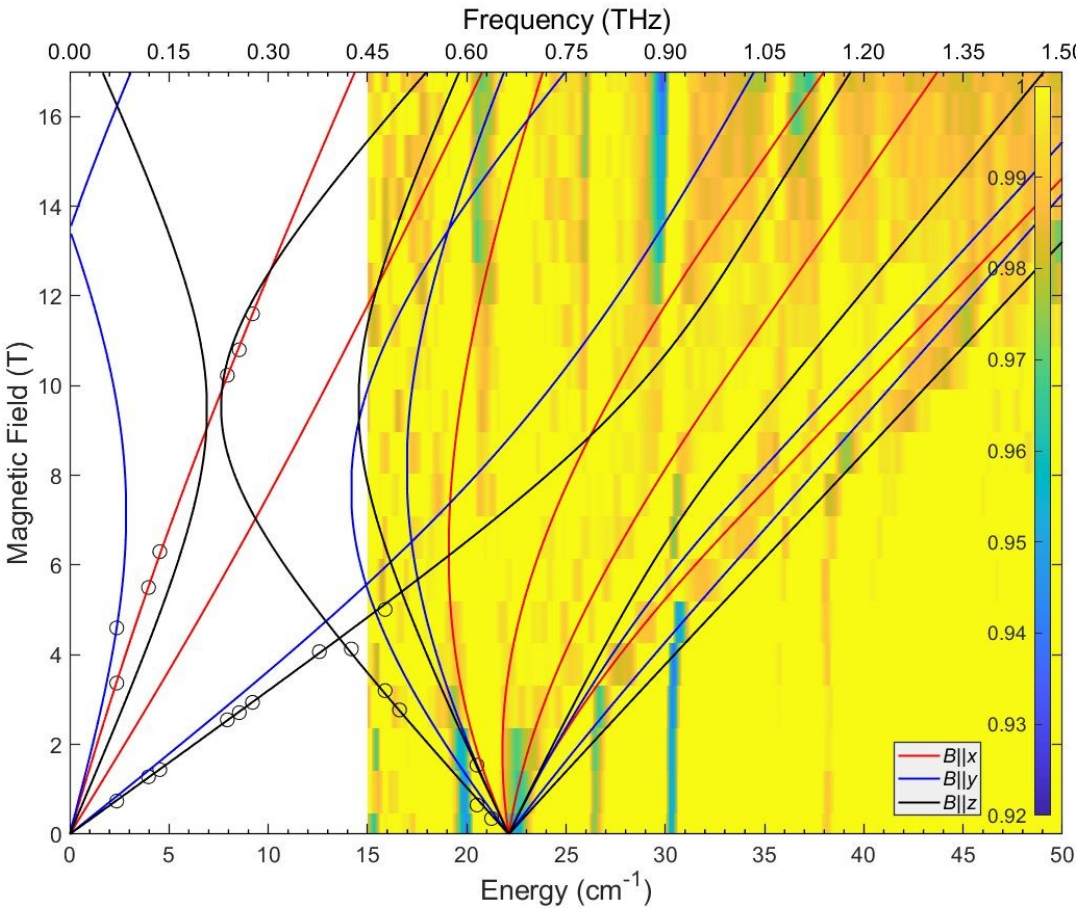

Fig. 4. A field vs. frequency dependence of the turning points in HFEPR spectra of **Co-N_3** as a pellet (open circles) with superimposed color curves representing turning points in the powder spectra simulated using the spin-Hamiltonian parameters in the text and *EasySpin*.[116] Red curves: $B_0 \parallel x$ when magnetic field is paralleled to the *x*-axis of the ZFS tensor, blue: $B_0 \parallel y$, black: $B_0 \parallel z$. The FIRMS heat map is overlayed to show a good agreement with HFEPR.

INS

Magnetic transitions are observed in inelastic neutron scattering (INS) by the interactions of the spins of incident neutrons and unpaired electrons of the sample. The neutron beam may also lead to excitations of vibrational levels giving the phonon spectrum. Variable-temperature (VT) INS performed on the Vibrational Spectrometer (VISION) at Spallation Neutron Source (SNS), Oak Ridge National Laboratory (ORNL), has provided the analysis of magnetic and phonon features. INS at VISION is not a magneto-spectroscopic technique, as, unlike HFEPR and FIRMS, no external magnet is used in the experiment. Instead, variable-temperature spectra

View Article Online
DOI: 10.1039/D5NJ01857A

and Bose-correction are used together to distinguish magnetic peaks from those of phonons, as discussed below.

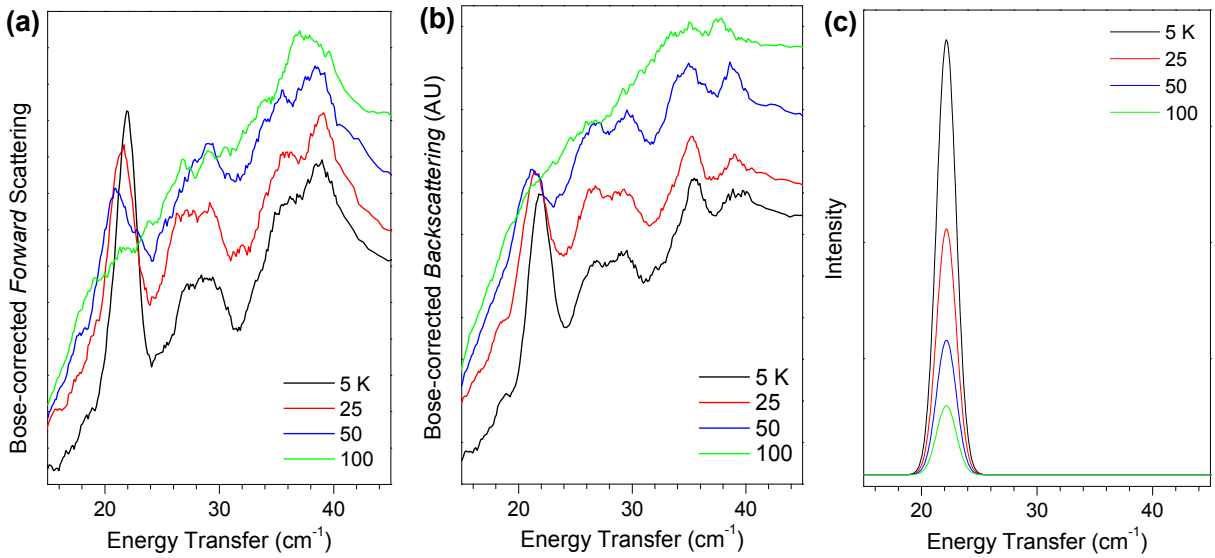

Fig. 5. (a) Bose-corrected, *forward*-scattering VT INS spectra of **Co-N_3**. (b) Bose-corrected, *backscattering* VT INS. AU = arbitrary unit, The spectra are Bose-corrected, a numerical frequency- and temperature-dependent normalization of phonons that follow Bose-Einstein statistics, highlighting magnetic spectral features that follow Boltzmann statistics.[108] (c) Bose-corrected theoretical VT INS spectra of an $S = 3/2$ spin system with $D = -10.39$ cm^{-1}, $|E| = 2.22$ cm^{-1}.

The forward (Fig. 5a) and backscattering (Fig. 5b) VT spectra reveal a clear magnetic transition in **Co-N_3** at 21.9(2) cm^{-1}. The magnetic transition is more intense in forward-scattering spectra in Fig. 5a than the backscattered spectra in Fig. 5b. This is because, in the forward INS spectra, scattered neutrons from magnetic interactions with the sample have lower scattering angles (i.e., low Q where $Q = |\vec{\boldsymbol{Q}}|$ is the length of the scattering vector of the momentum transfer $\vec{\boldsymbol{Q}}$ during neutron scattering[108]) than in backscattered spectra. Magnetic transitions are stronger in low-Q scattered neutrons than in high-Q scattered neutrons. In contrast, phonon/vibrational peaks are weaker in low-Q scattered neutrons but stronger in high-Q scattered neutrons.

Theoretical VT INS spectra of the magnetic peak for an $S = 3/2$ spin system with $D = -10.39$ cm^{-1} and $|E| = 2.22$ cm^{-1} in Fig. 5c, calculated based on Eq. 1 (in the Experimental Section and Calculations), show the observed INS peak at 21.9(2) cm^{-1} matches the calculated peak,

View Article Online
DOI: 10.1039/D5NJ01857A

especially the changes with temperatures. The comparison supports the assignment of this peak to be magnetic in nature. In other words, the peak represents excitation from the $M_S = |\pm 3/2\rangle$ level to the $|\pm 1/2\rangle$ level. The assignment of the INS peak at 21.9(2) cm^{-1} in Fig. 5a-b requires no use of magnetic field in contrast to FIRMS spectra in Fig. 2. That is, the INS spectra in Fig. 5a-b are truly from a zero-field experiment. This feature decreases in intensity as temperature increases due to the depopulation of the ground magnetic state.

DC and AC magnetometry studies

Magnetometry is extensively used to study the properties of molecular magnetism. However, this technique is sensitive to sample weight and centering which may cause fluctuations in the magnitude of the data, and consequently the SH parameter obtained though data fittings may be inaccurate. Chen and coworkers reported DC magnetometry fits of the second polymorph **Co-N_3'**.[54] We have used magnetometry as a common technique to compare our results on the first polymorph **Co-N_3** with those reported for **Co-N_3'** as well as with those from the advanced spectroscopies. These results are listed in Table 1.

DC magnetometry

Variable-temperature (VT) DC magnetic susceptibility of **Co-N_3** with an applied field of 0.1 T at 2-300 K gives the results shown in Fig. 6. At 300 K, the $\chi_M T$ value of 2.11 cm^3 K mol^{-1} is greater than the spin-only value [$\chi_M T = (N\beta^2 g^2/3k_B)S(S+1) = 1.875$ cm^3 mol^{-1} K] of a high-spin Co^{II} ion with $S = 3/2$ and $g = 2$, confirming the presence of unquenched orbital contribution to the magnetic moment. Experimental DC magnetometry is compared with the simulated traces (Fig. 6) defined by the SH parameters obtained by HFEPR. The low temperature downturn of the simulated $\chi_M T$ trace is in good agreement with the experimental, indicating that the anisotropy is well defined. However, the simulated $\chi_M T = 2.49$ cm^3 mol^{-1} K at 300 K deviates from the experimental data but is closer to the previously reported (2.51 cm^3 mol^{-1} K) of **Co-N_3**. Simulation of the DC data gave $D = -9.31(10)$ cm^{-1}, $|E| = 0.5(4)$ cm^{-1} [$|E/D| = 0.04(5)$], and $g_{iso} = 2.12$, which are given in Table 1 for comparison. The D and g values are slightly different from those by HFEPR. Such differences are common,[19, 67, 68, 80, 110, 117-121] highlighting the need to use advanced spectroscopies to determine the spin-Hamiltonian parameters. The reduced

View Article Online
DOI: 10.1039/D5NJ01857A

magnetization at 7 T and 1.8 K is 2.47$N\beta$, in which the magnetic saturation has yet to be achieved. The non-superposition of the variable-field curves further indicates the presence of considerable magnetic anisotropies and (besides the scaling) the relative positions of the simulated magnetization curves are also in good agreement with experimental results.

The SH parameters of the **Co-N$_3$** and **Co-N$_3$'** in Table 1 suggest that they have slightly different magnetic properties. The *SHAPE* analyses [which is the calculation of continuous shape measures (CShM) of set atomic positions relative to an ideal geometry][122] indicate differentiating deviations from ideal T_d symmetry, where the **Co-N$_3$** has the smaller deviation. From this analysis, **Co-N$_3$** is inferred to have slightly smaller anisotropy, which is reflected in its smaller D value and zero-field splitting [ZFS. $2D' = 2(D^2 + 3E^2)^{1/2} = 18.7(4)$ cm^{-1}] than the second polymorph **Co-N$_3$'** ($2D' = 24$ cm^{-1}) in Table 1. Both studies determined the sign of D to be negative, corresponding to axial anisotropy. Deviation caused by subtle changes in anisotropy cannot be discerned, while inaccuracies in magnetometry exist.

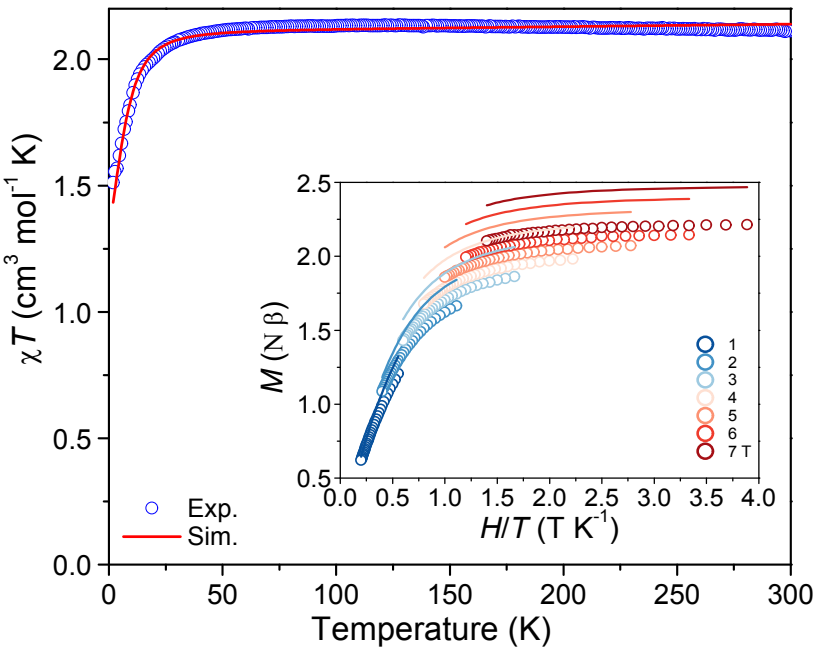

Fig. 6. DC magnetic susceptibility of **Co-N$_3$** at 0.1 T. The inset is the reduced magnetization at varying magnetic fields. The solid lines are *PHI* simulations, giving spin-Hamiltonian parameters in Table 1.

View Article Online
DOI: 10.1039/D5NJ01857A

Table 1. Summary of magnetic parameters determined by different techniques and *SHAPE* analyses for **Co-N_3** in comparison with the reported **Co-N_3'**

Complex	Method	D (cm^{-1})	$\|E\|$ (cm^{-1})	$\|E/D\|$	$ZFS = 2D'$ (cm^{-1})	g	*SHAPE*
Co-N_3	HFEPR	−10.39(5)	2.22(7)	0.21(1)	22.2(1)	[2.21(4), 2.35(11), 2.35(2)]	0.107
	FIRMS				22(1)		
	INS				21.9(2)		
	DC magnetometry	-9.31(10)	0.5(4)	0.04(5)	18.7(4)	2.12	
Co-N_3'	DC magnetometry in Ref. 54	-12.11(5)	0.49(7)	0.04(1)	24.3(1)	2.31	0.399

AC magnetometry

The AC susceptibility of **Co-N_3** was used to probe dynamic magnetization. VT AC susceptibility under a static DC magnetic field of 0.06 T is shown in Fig. 7. Out-of-phase (χ_M'') signals are present under an applied DC field (Fig. 7-Top), which is an indication of field-induced slow magnetic relaxation. Signals below 3 K become strongly dependent on temperature. However, no obvious maxima of χ_M'' was observed, preventing further analysis of the relaxation process. The AC susceptibility is compatible to that of **Co-N_3'**.[54]

It should be pointed out that the polymorph **Co-N_3'** was characterized by DC and AC susceptibility. Its SH parameters were derived based on indirect fitting of the DC susceptibility data. In contrast, for **Co-N_3**, the ZFS transitions were directly observed by FIRMS and INS, in addition to SH parameters being independently determined by tunable-frequency HFEPR and DC susceptibility data.

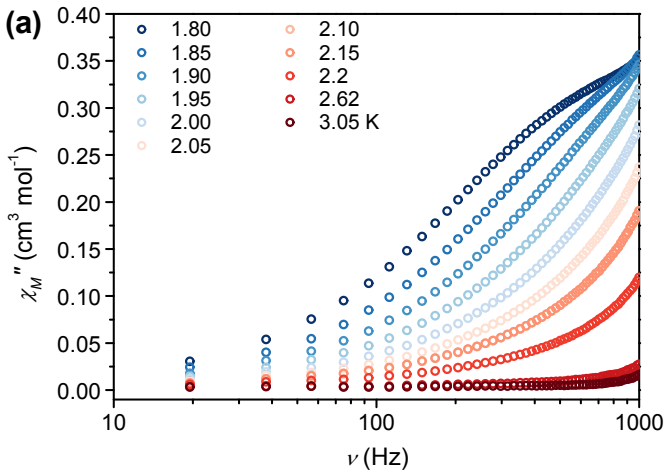

View Article Online
DOI: 10.1039/D5NJ01857A

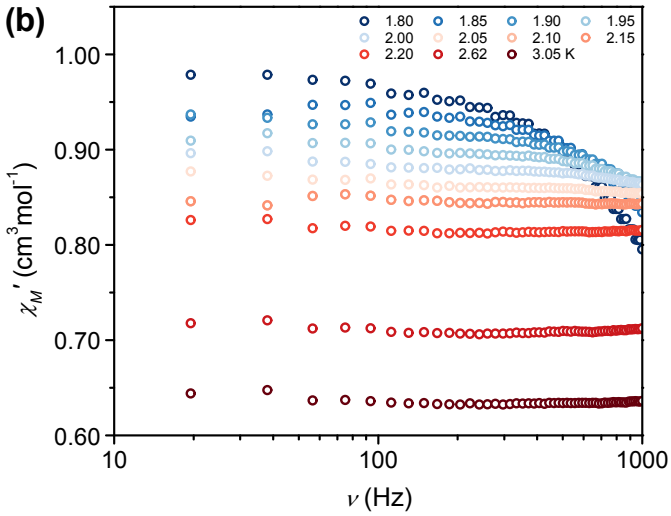

Fig. 7. Frequency-dependent, (a) out-of-phase and (b) in-phase AC magnetic susceptibility of **Co-N$_3$** at 0.06 T DC field.

Analysis of d-orbitals and ZFS by Ligand Field Theory

Semiempirical ligand field theory (LFT) with the angular overlap model (AOM) approach[123-126] has been used to understand the origin of ZFS in the two polymorphs. These calculations were performed on the locally written (J. Telser) program DDN.[127] We also compare the results of DDN to those from Ligfield[128] and they agree to within the third decimal place in cm^{-1} or better.

We define a set of parameters that reproduce the experimental ZFS of **Co-N$_3$**: ζ = –495 cm^{-1}, B = 919 cm^{-1}, C = 3917 cm^{-1}, ε_σ = 7000 cm^{-1}, $\varepsilon_{\pi s}$ = 2900 cm^{-1}, and $\varepsilon_{\pi c}$ = 1800 cm^{-1}, where B and C are Racah parameters, and ε_σ and ε_π are the σ and π bonding energies. The values of ζ and B are 93% of the free-ion value, whereas C is obtained by using the free-ion C/B ratio of 4.26. Next, we define angles (θ, ϕ) that represent the ligand positions relative to a principal axis (d_z^2 orbital) illustrated in Fig. S6, as in the crystal structures of **Co-N$_3$** and **Co-N$_3$'**. The results are compared with "ideal" symmetries of T_d, C_{2v}, and D_{2d} in Table S1. The relative d-orbital splitting (Fig. 8) and ZFS (Fig. 9) are then evaluated for each structure/geometry. The LFT models of **Co-N$_3$** and **Co-N$_3$'** are found to have the same d-orbital splitting. The calculations with the T_d geometry yielded the lowest ZFS value and gave degenerate doublet ground state ($d_{x^2-y^2}$, d_{z^2}) and triplet excited state (d_{xy}, d_{xz}, d_{yz}). The C_{2v} distortion slightly raises the d_{xy} and $d_{x^2-y^2}$ while lowering the d_{xz} and d_{yz} orbitals. The D_{2d} distortion provides the closest d-orbital energies to the

View Article Online
DOI: 10.1039/D5NJ01857A

actual structures, while providing degeneracy amongst the d_{xz} and d_{yz} orbitals. The metal orbitals increase in energy when they have better overlaps with ligand orbitals. The ZFS energy predicted via models shows a significant increase from T_d to D_{2d}, where the polymorphs are the closest to D_{2d}. The two polymorphs are also found to have the same ZFS energy from the ligand field theory calculations. The ground total S for **Co-N$_3$** and **Co-N$_3$'** are found close to 3/2, indicating axial anisotropy.

The d^7 120 × 120 microstates matrix, including interelectronic (Racah parameters), spin-orbit coupling, and AOM bonding parameters, is diagonalized to give the energies. The eigenvectors give the orbital configurations in the m_l basis set. The basis function is the Slater determinants for in this case d^7 in the $|L, m_L, S, m_S>$ basis set. These are given for $|L, 0, S, +1/2>$ by Slater in Ref. 129.

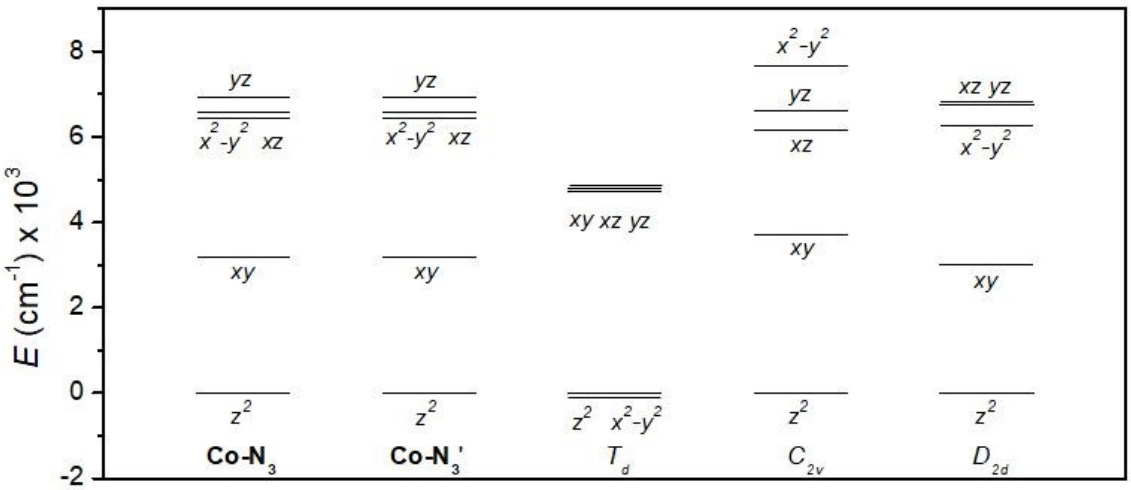

Fig. 8. *d*-orbital splitting of the structures **Co-N$_3$** and **Co-N$_3$'** and distortions to "ideal" symmetries.

View Article Online
DOI: 10.1039/D5NJ01857A

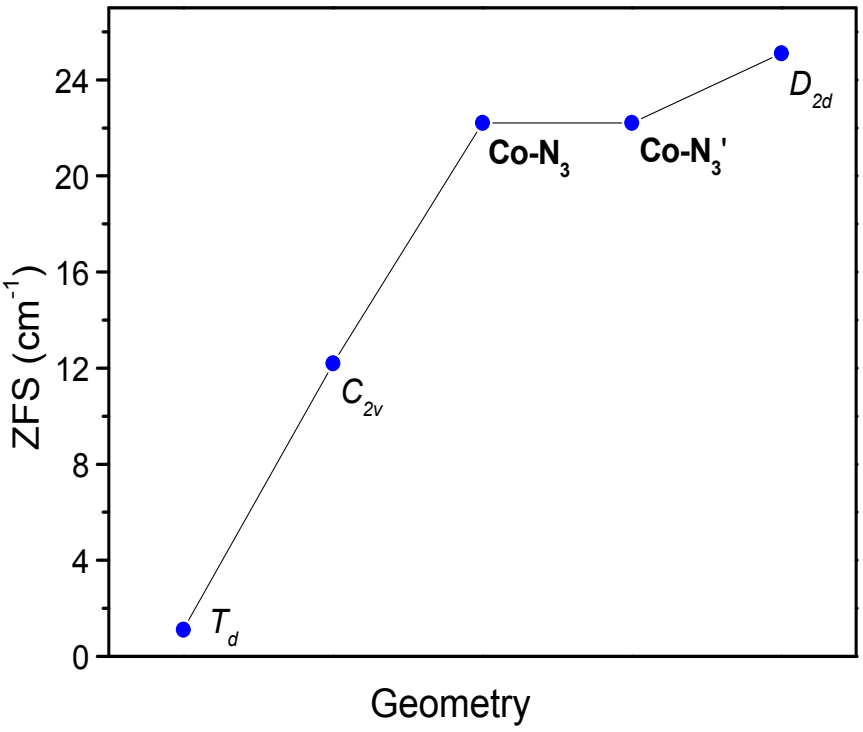

Fig. 9. Trend in calculated ZFS energy for the structures of **Co-N_3** and **Co-N_3'** and distortions to "ideal" symmetries.

Conclusions

We have investigated the magnetic properties of $(PPh_4)_2[Co(N_3)_4]$ (**Co-N_3**) and compared those with its polymorph (**Co-N_3'**). Advanced spectroscopic techniques (FIRMS, HFEPR, and INS) allow the determination of ZFS and spin Hamiltonian (SH) parameters with easy-axis anisotropy. The current work is a rare example that magnetic properties of a metal complex (a polymorph in this case) have been probed by both magnetometry and several advanced spectroscopies, demonstrating the critical role that the spectroscopies play in determining precise SH parameters. *SHAPE* analyses show the differences in the two polymorphs, likely contributing to deviations in their magnetic anisotropies. The LFT calculations provide an understanding of the origin of ZFS in the two polymorphs. Calculated ZFS energy for the "ideal" D_{2d} symmetry is the closest to the actual structures than T_d symmetry. AC magnetometry reveals the complex to be a field-induced SIM with slow magnetic relaxation. The work adds to the studies showing that homoleptic Co^{2+} complexes with distorted T_d symmetry, such as **Co-N_3**, still give sizable ZFS and could be SIM candidates.

View Article Online
DOI: 10.1039/D5NJ01857A

Experimental section and calculations

Synthesis of $(PPh_4)_2[Co(N_3)_4]$

The reactant $(PPh_4)_2[CoCl_4]$ was synthesized according to the published procedure in air.[54] The complex $(PPh_4)_2[Co(N_3)_4]$ was prepared by modifying the original procedure.[54, 130] An excess of NaN_3 (0.51 g, 7.7 mmol) was slowly added to a solution of $(PPh_4)_2[CoCl_4]$ (0.25 g, 0.28 mmol) in acetone (10 mL) with 5% water. The reaction was stirred for 1.5 h, and then the volume of solution is reduced approximately in half by blowing N_2 over the solution. The remaining solution is filtered to remove the excess NaN_3, and CCl_4 is added to the filtrate to precipitate the resulting blue solid of **Co-N_3** (0.177 g, 0.195 mmol, 68%). The complex was confirmed by PXRD (Fig. S3) to have the reported crystal structure published by Sen and coworkers.[61] FT-IR of the solid is given in Fig. S5, respectively. An admixture of the two polymorphic complexes was also observed in some cases by PXRD (Fig. S4). But only the sample of the first polymorph **Co-N_3** was used in the current studies.

FIRMS

FIRMS spectra were collected at National High Magnetic Field Laboratory (NHMFL) using a Bruker Vertex 80v Fourier-transform infrared (FT-IR) spectrometer coupled with a 17.5 T vertical-bore superconducting magnet. The experimental setup is equipped with a mercury lamp and a composite silicon bolometer (Infrared Laboratories), as an incoherent (sub)-THz radiation source and detector, respectively. The THz radiation propagates in freespace inside the optical beamline, connecting the output of the spectrometer and top of the sample probe. The radiation then passes through the brass lightpipe through a 2.5 m distance to the field center. The probe and beamline are evacuated to eliminate strong parasitic absorptions of the air. The samples are mulls of n-eicosane and powder (~2 mg) of each complex. Both the sample and the bolometer were cooled by low pressure helium gas to ~5 K. The spectrum of the THz radiation transmitted through the samples was measured between 10 and 720 cm^{-1} (0.3–21.6 THz) with a 50 μm beamsplitter, mid-IR globar source, resolution of 0.3 cm^{-1} (9 GHz), acquisition time of 3 min, 20 kHz scanner speed, and 200 gain.

HFEPR

HFEPR was performed at the EMR facility at NHMFL. The facility operates a

View Article Online
DOI: 10.1039/D5NJ01857A

transmission spectrometer described elsewhere,[131] which was modified by the use of Virginia Diodes Inc. (VDI, Charlottesville, VA, USA) sources, generating sub-THz radiation in the 50–640 GHz frequency range. The spectrometer is associated with a 15/17 T warm-bore superconducting magnet. The samples were measured both "as is" which allowed them to orient (torque) in the magnetic field, or as pellets mixed with n-eicosane. About 30–60 mg of the powder samples was used in each measurement. HFEPR spectra were typically collected at 5–10 K. The spectra of **Co-N_3** were simulated using the software package SPIN available freely from Dr. A. Ozarowski (NHMFL) at https://osf.io/z72tg/.

INS

Variable-temperature (VT) INS spectra were collected on VISION at ORNL. For each measurement, approximately 0.5 g of the powder sample was sealed in a vanadium can within a helium environment. The vanadium can was then fixed on the end of the sample stick and lowered inside the neutron beam within a JANIS closed-cycle refrigerator (CCR). VISION has two detector banks, forward- and backward-scattering, providing data for low- and high-scattering angles, respectively. Magnetic transitions are more intense by the forward scattering detectors for their low scattering angle dependence. VISION is an indirect-geometry INS spectrometer.[108] VT INS were measured at 5.0(5), 25.0(5), 50.0(5), and 100.0(5) K. Phonon population effect was corrected by normalizing the INS intensity at energy transfer ω with $\coth\left(\frac{\hbar\omega}{2k_BT}\right)$.[95]

Magnetic neutron scattering cross-section corresponds to the number of neutrons scattered per second into a solid angle $d\Omega$ with energy transfer between $\hbar\omega$ and $\hbar(\omega + d\omega)$, divided by the flux of the incident neutrons. For spin-only scattering using unpolarized neutrons[132] from a mononuclear complex, the magnetic scattering cross-section is expressed by Eq. 5:[133, 134]

$$\frac{d^2\sigma}{d\Omega d\omega} = (\gamma r_0)^2 \frac{k_f}{k_i}\left[\frac{1}{2} g\, F(\vec{\boldsymbol{Q}})\right]^2 e^{-2W(\vec{\boldsymbol{Q}})} \sum_{\alpha,\beta}\left(\delta_{\alpha\beta} - \frac{\vec{\boldsymbol{Q}}_\alpha \cdot \vec{\boldsymbol{Q}}_\beta}{Q^2}\right) S^{\alpha\beta}(\vec{\boldsymbol{Q}}, \omega) \qquad (5)$$

where σ = neutron cross section; γ = gyromagnetic ratio of neutron, r_0 = classical radius of an electron, g = Landé g-factor, $F(\vec{\boldsymbol{Q}})$ = dimensionless magnetic form factor defined as the Fourier

View Article Online
DOI: 10.1039/D5NJ01857A

transform of the normalized spin density associated with magnetic ions, $e^{-2W(\vec{Q})}$ = Debye-Waller factor caused by thermal motion, $S^{\alpha\beta}(\vec{Q},\omega)$ = magnetic scattering function, $\left(\delta_{\alpha\beta} - \frac{\vec{Q}_\alpha \vec{Q}_\beta}{Q^2}\right)$ = polarization factor which implies neutrons can only couple to magnetic moments or spin fluctuations perpendicular to $\vec{Q}$, ω = energy change experienced by the sample, ω = angular frequency of neutron, and α, β = Cartesian coordinates *x, y, z*.

Magnetic peak position in INS spectra gives a direct measurement of the eigenvalues of the spin Hamiltonian in Eq. 1. Simulated INS spectra were obtained by calculating the energies and corresponding wave functions via exact diagonalization of the spin Hamiltonian in Eq. 1. These calculations can be used to get the INS intensity, which is proportional to the magnetic scattering function $S^{\alpha\beta}(\vec{Q},\omega)$.

DC/AC magnetometry measurements

DC measurements were collected at the University of South Carolina using a PPMS DynaCool by Quantum Design. AC measurements were collected at Oak Ridge National Laboratory (ORNL) using a Quantum Design MPMS-3. Powder sample (approximately 20 mg) were held in neat pellet form in a polypropylene straw. Pascal's constants were applied to correct for diamagnetic contribution.[135]

Analysis of d-orbitals and ZFS by Ligand Field Theory

These calculations were performed on the locally written (J. Telser) program DDN.[127] Additional results from the ligand field analyses, including a summary of the ligand field and AOM parameters are given in Supporting Information (Fig. S6 and Tables S1-S6).

Data availability

Data are available from the authors upon request. The authors confirm that the data supporting the findings of this study are available within the article and its ESI.

Associate content

ESI including author contributions, additional HFEPR, powder X-ray diffraction data and

View Article Online
DOI: 10.1039/D5NJ01857A

FT-IR spectra of the sample, additional results from the Ligand Field Theory analyses, additional discussion of the Bose correction, and codes for the simulation of spin = 3/2 magnetic transitions in INS.

Conflicts of interest

The authors declare no competing financial interest.

Acknowledgments

US National Science Foundation [CHE-2055499 and CHE-2349345 to Z.-L.X. and DGE-2152159 for an NRT (Research Traineeship Program) fellowship to A.T.H.] is acknowledged for the support of the research. Both DC and AC magnetic property studies was conducted in part by J.X. and R.J. supported by Grant No. DE-SC0024501 funded by the U.S. Department of Energy, Office of Science and in part at the Center for Nanophase Materials Sciences, which was sponsored at Oak Ridge National Laboratory by the Scientific User Facilities Division, Office of Basic Energy Sciences, U.S. Department of Energy. We thank Dr. A. Ozarowski for his EPR software package SPIN. Part of this work was performed at the National High Magnetic Field Laboratory which is supported by NSF Cooperative Agreement No. DMR-2128556 and the State of Florida. Neutron scattering experiments were conducted at the VISION beamline at ORNL's Spallation Neutron Source, which is supported by the Scientific User Facilities Division, Office of Basic Energy Sciences (BES), U.S. Department of Energy (DOE), under Contract No. DE-AC0500OR22725 with UT Battelle, LLC. The authors thank Michael J. Jenkins and Miranda A. Phillips for assistance.

View Article Online
DOI: 10.1039/D5NJ01857A

References

1. A. K. Bar, C. Pichon and J.-P. Sutter, Magnetic Anisotropy in Two- to Eight-Coordinated Transition-Metal Complexes: Recent Developments in Molecular Magnetism. *Coord. Chem. Rev.*, 2016, **308**, 346-380. https://doi.org/10.1016/j.ccr.2015.06.013.
2. C. Benelli and D. Gatteschi, *Introduction to Molecular Magnetism: From Transition Metals to Lanthanides*, Wiley-VCH, Weinheim, Germany, 1st edn., 2015. http://doi.org/10.1002/anie.201511481.
3. H. Andres, R. Basler, H.-U. Güdel, G. Aromí, G. Christou, H. Büttner and B. Rufflé, Inelastic neutron scattering and magnetic susceptibilities of the single-molecule magnets $[Mn_4O_3X(OAc)_3(dbm)_3]$ (X = Br, Cl, OAc, and F): Variation of the anisotropy along the series. *J. Am. Chem. Soc.*, 2000, **122**, 12469-12477. http://doi.org/10.1021/ja0009424.
4. M. Feng and M.-L. Tong, Single Ion Magnets from 3*d* to 5*f*: Developments and Strategies. *Chem. Eur. J.*, 2018, **24**, 7574-7594. https://doi.org/10.1002/chem.201705761.
5. B. N. Figgis, J. Lewis and F. E. Mabbs, The Magnetic Properties of Some d^3-complexes. *J. Chem. Soc.*, 1961, DOI: 10.1039/JR9610003138, 3138-3145. http://doi.org/10.1039/JR9610003138.
6. J. M. Frost, K. L. M. Harriman and M. Murugesu, The Rise of 3*d* Single-Ion Magnets in Molecular Magnetism: Towards Materials from Molecules? *Chem. Sci.*, 2016, **7**, 2470-2491. http://doi.org/10.1039/C5SC03224E.
7. S. Gao, *Molecular Nanomagnets and Related Phenomena*, Springer, Berlin, 2015. http://doi.org/10.1007/978-3-662-45723-8.
8. D. Gatteschi, R. Sessoli and J. Villain, *Molecular Nanomagnets*, Oxford University Press, Oxford; New York, 2006. https://doi.org/10.1093/acprof:oso/9780198567530.001.0001.
9. S. Gomez-Coca, A. Urtizberea, E. Cremades, P. J. Alonso, A. Camon, E. Ruiz and F. Luis, Origin of Slow Magnetic Relaxation in Kramers Ions with Non-uniaxial Anisotropy. *Nat. Commun.*, 2014, **5**, 4300. https://doi.org/10.1038/ncomms5300.
10. M. Holynska, *Single-Molecule Magnets: Molecular Architectures and Building Blocks for Spintronics*, Wiley-VCH, Weinheim, Germany, 2019. https://doi.org/10.1002/9783527809929.
11. S. T. Liddle and J. van Slageren, Improving *f*-element Single Molecule Magnets. *Chem. Soc. Rev.*, 2015, **44**, 6655-6669. http://doi.org/10.1039/C5CS00222B.

View Article Online
DOI: 10.1039/D5NJ01857A

12. J. Lu, M. Guo and J. Tang, Recent Developments in Lanthanide Single-Molecule Magnets. *Chem. Asian J.*, 2017, **12**, 2772-2779. https://doi.org/10.1002/asia.201701032.

13. E. J. L. McInnes and R. E. P. Winpenny, *Molecular Magnets*, in *Comp. Inorg. Chem. II*, ed. K. Poeppelmeier, Elsevier, Amsterdam, 2013. https://doi.org/10.1016/B978-0-08-097774-4.00419-8.

14. A. Sarkar, S. Dey and G. Rajaraman, Role of Coordination Number and Geometry in Controlling the Magnetic Anisotropy in Fe^{II}, Co^{II}, and Ni^{II} Single-Ion Magnets. *Eur. J. Chem.*, 2020, **26**, 14036-14058. https://doi.org/10.1002/chem.202003211.

15. Y. P. Tupolova, I. N. Shcherbakov, D. V. Korchagin, V. V. Tkachev, V. E. Lebedev, L. D. Popov, K. V. Zakharov, A. N. Vasiliev, A. V. Palii and S. M. Aldoshin, Fine-Tuning of Uniaxial Anisotropy and Slow Relaxation of Magnetization in the Hexacoordinate Co(II) Complexes with Acidoligands. *J. Phys. Chem. C*, 2020, **124**, 25957-25966. https://doi.org/10.1021/acs.jpcc.0c07552.

16. X.-Y. Wang, C. Avendaño and K. R. Dunbar, Molecular Magnetic Materials Based on 4d and 5d Transition Metals. *Chem. Soc. Rev.*, 2011, **40**, 3213-3238. http://doi.org/10.1039/C0CS00188K.

17. A. Zabala-Lekuona, J. M. Seco and E. Colacio, Single-Molecule Magnets: From Mn_{12}-ac to dysprosium metallocenes, a travel in time. *Coord. Chem. Rev.*, 2021, **441**, 213984. https://doi.org/10.1016/j.ccr.2021.213984.

18. Z. Zhuo, G.-L. Li and Y.-G. Huang, *Understanding Magneto-Structural Correlations Toward Design of Molecular Magnets*, in *Advanced Structural Chemistry, Vol. 2*, ed. R. Cao, 2021, pp. 777-832. https://doi.org/10.1002/9783527831753.ch13.

19. A. N. Bone, C. N. Widener, D. H. Moseley, Z. Liu, Z. Lu, Y. Cheng, L. L. Daemen, M. Ozerov, J. Telser, K. Thirunavukkuarasu, D. Smirnov, S. M. Greer, S. Hill, J. Krzystek, K. Holldack, A. Aliabadi, A. Schnegg, K. R. Dunbar and Z.-L. Xue, Applying Unconventional Spectroscopies to the Single-Molecule Magnets $Co(PPh_3)_2X_2$ (X = Cl, Br, I): Unveiling Magnetic Transitions and Spin-Phonon Coupling. *Eur. J. Chem.*, 2021, **27**, 11110-11125. https://doi.org/10.1002/chem.202100705.

20. P. Tin, A. N. Bone, N. N. Bui, Y.-Q. Zhang, T. Chang, D. H. Moseley, M. Ozerov, J. Krzystek, Y. Cheng, L. L. Daemen, X. Wang, L. Song, Y.-S. Chen, D. Shao, X.-Y. Wang, X.-T. Chen and Z.-L. Xue, Advanced Spectroscopic and Computational Studies of

View Article Online
DOI: 10.1039/D5NJ01857A

a Cobalt(II) Coordination Polymer with Single-Ion-Magnet Properties. *J. Phys. Chem. C*, 2022, **126**, 13268-13283. https://doi.org/10.1021/acs.jpcc.2c03083.

21. J. Ferrando-Soria, J. Vallejo, M. Castellano, J. Martínez-Lillo, E. Pardo, J. Cano, I. Castro, F. Lloret, R. Ruiz-García and M. Julve, Molecular magnetism, quo vadis? A historical perspective from a coordination chemist viewpoint. *Coord. Chem. Rev.*, 2017, **339**, 17-103. https://doi.org/10.1016/j.ccr.2017.03.004.
22. A. Świtlicka, B. Machura, J. Cano, F. Lloret and M. Julve, A Study of the Lack of Slow Magnetic Relaxation in Mononuclear Trigonal Bipyramidal Cobalt (II) Complexes. *ChemistrySelect*, 2021, **6**, 576-582. https://doi.org/10.1002/slct.202100061.
23. P. S. Perlepe, D. Maniaki, E. Pilichos, E. Katsoulakou and S. P. Perlepes, Smart Ligands for Efficient 3d-, 4d- and 5d-Metal Single-Molecule Magnets and Single-Ion Magnets. *Inorganics*, 2020, **8**, 39. https://doi.org/10.3390/inorganics8060039.
24. D. Shao and X.-Y. Wang, Development of Single-Molecule Magnets. *Chin. J. Chem.*, 2020, **38**, 1005-1018. https://doi.org/10.1002/cjoc.202000090.
25. C. A. P. Goodwin, Blocking like it's hot: a synthetic chemists' path to high-temperature lanthanide single molecule magnets. *Dalton Trans.*, 2020, **49**, 14320-14337. https://doi.org/10.1039/D0DT01904F.
26. P. Kumar Sahu, R. Kharel, S. Shome, S. Goswami and S. Konar, Understanding the Unceasing Evolution of Co(II) Based Single-Ion Magnets. *Coord. Chem. Rev.*, 2023, **475**, 214871. https://doi.org/10.1016/j.ccr.2022.214871.
27. S. Ziegenbalg, D. Hornig, H. Görls and W. Plass, Cobalt(II)-Based Single-Ion Magnets with Distorted Pseudotetrahedral [N2O2] Coordination: Experimental and Theoretical Investigations. *Inorg. Chem.*, 2016, **55**, 4047-4058. https://doi.org/10.1021/acs.inorgchem.6b00373.
28. S. Vaidya, A. Upadhyay, S. K. Singh, T. Gupta, S. Tewary, S. K. Langley, J. P. S. Walsh, K. S. Murray, G. Rajaraman and M. Shanmugam, A synthetic strategy for switching the single ion anisotropy in tetrahedral Co(ii) complexes. *Chem. Commun.*, 2015, **51**, 3739-3742. http://doi.org/10.1039/C4CC08305A.
29. L. Smolko, J. Černák, M. Dušek, J. Miklovič, J. Titiš and R. Boča, Three tetracoordinate Co(II) complexes [Co(biq)X_2] (X = Cl, Br, I) with easy-plane magnetic anisotropy as

View Article Online
DOI: 10.1039/D5NJ01857A

field-induced single-molecule magnets. *Dalton Trans.*, 2015, **44**, 17565-17571. http://doi.org/10.1039/C5DT02827B.

30. L. Smolko, J. Černák, M. Dušek, J. Titiš and R. Boča, Tetracoordinate Co(II) complexes containing bathocuproine and single molecule magnetism. *New J. Chem.*, 2016, **40**, 6593-6598. http://doi.org/10.1039/C6NJ00372A.
31. L. Smolko, J. Černák, J. Kuchár, C. Rajnák, J. Titiš and R. Boča, Field-Induced Slow Magnetic Relaxation in Mononuclear Tetracoordinate Cobalt(II) Complexes Containing a Neocuproine Ligand. *Eur. J. Inorg. Chem.*, 2017, **2017**, 3080-3086. https://doi.org/10.1002/ejic.201700293.
32. A. Świtlicka, B. Machura, R. Kruszynski, J. Cano, L. M. Toma, F. Lloret and M. Julve, The influence of pseudohalide ligands on the SIM behaviour of four-coordinate benzylimidazole-containing cobalt(II) complexes. *Dalton Trans.*, 2018, **47**, 5831-5842. http://doi.org/10.1039/C7DT04735E.
33. S. Vaidya, P. Shukla, S. Tripathi, E. Rivière, T. Mallah, G. Rajaraman and M. Shanmugam, Substituted versus Naked Thiourea Ligand Containing Pseudotetrahedral Cobalt(II) Complexes: A Comparative Study on Its Magnetization Relaxation Dynamics Phenomenon. *Inorg. Chem.*, 2018, **57**, 3371-3386. https://doi.org/10.1021/acs.inorgchem.8b00160.
34. J. M. Zadrozny and J. R. Long, Slow Magnetic Relaxation at Zero Field in the Tetrahedral Complex $[Co(SPh)_4]^{2-}$. *J. Am. Chem. Soc.*, 2011, **133**, 20732-20734. https://doi.org/10.1021/ja2100142.
35. J. M. Zadrozny, J. Telser and J. R. Long, Slow magnetic relaxation in the tetrahedral cobalt(II) complexes $[Co(EPh)_4]^{2-}$ (EO, S, Se). *Polyhedron*, 2013, **64**, 209-217. https://doi.org/10.1016/j.poly.2013.04.008.
36. E. A. Suturina, J. Nehrkorn, J. M. Zadrozny, J. Liu, M. Atanasov, T. Weyhermüller, D. Maganas, S. Hill, A. Schnegg, E. Bill, J. R. Long and F. Neese, Magneto-Structural Correlations in Pseudotetrahedral Forms of the $[Co(SPh)_4]^{2-}$ Complex Probed by Magnetometry, MCD Spectroscopy, Advanced EPR Techniques, and ab Initio Electronic Structure Calculations. *Inorg. Chem.*, 2017, **56**, 3102-3118. https://doi.org/10.1021/acs.inorgchem.7b00097.

View Article Online
DOI: 10.1039/D5NJ01857A

37. M. S. Fataftah, J. M. Zadrozny, D. M. Rogers and D. E. Freedman, A Mononuclear Transition Metal Single-Molecule Magnet in a Nuclear Spin-Free Ligand Environment. *Inorg. Chem.*, 2014, **53**, 10716-10721. https://doi.org/10.1021/ic501906z.

38. S. Vaidya, S. Tewary, S. K. Singh, S. K. Langley, K. S. Murray, Y. Lan, W. Wernsdorfer, G. Rajaraman and M. Shanmugam, What Controls the Sign and Magnitude of Magnetic Anisotropy in Tetrahedral Cobalt(II) Single-Ion Magnets? *Inorg. Chem.*, 2016, **55**, 9564-9578. https://doi.org/10.1021/acs.inorgchem.6b01073.

39. S. Sottini, G. Poneti, S. Ciattini, N. Levesanos, E. Ferentinos, J. Krzystek, L. Sorace and P. Kyritsis, Magnetic Anisotropy of Tetrahedral Co^{II} Single-Ion Magnets: Solid-State Effects. *Inorg. Chem.*, 2016, **55**, 9537-9548. https://doi.org/10.1021/acs.inorgchem.6b00508.

40. D. Tu, D. Shao, H. Yan and C. Lu, A carborane-incorporated mononuclear Co(II) complex showing zero-field slow magnetic relaxation. *Chem. Commun.*, 2016, **52**, 14326-14329. http://doi.org/10.1039/C6CC07728E.

41. D. R. Alcoba, O. B. Oña, G. E. Massaccesi, A. Torre, L. Lain, J. I. Melo, J. E. Peralta and J. M. Oliva-Enrich, Magnetic Properties of Mononuclear Co(II) Complexes with Carborane Ligands. *Inorg. Chem.*, 2018, **57**, 7763-7769. https://doi.org/10.1021/acs.inorgchem.8b00815.

42. K. Chattopadhyay, M. J. Heras Ojea, A. Sarkar, M. Murrie, G. Rajaraman and D. Ray, Trapping of a Pseudotetrahedral $Co^{II}O_4$ Core in Mixed-Valence Mixed-Geometry $[Co_5]$ Coordination Aggregates: Synthetic Marvel, Structures, and Magnetism. *Inorg. Chem.*, 2018, **57**, 13176-13187. https://doi.org/10.1021/acs.inorgchem.8b01577.

43. X.-N. Yao, M.-W. Yang, J. Xiong, J.-J. Liu, C. Gao, Y.-S. Meng, S.-D. Jiang, B.-W. Wang and S. Gao, Enhanced magnetic anisotropy in a tellurium-coordinated cobalt single-ion magnet. *Inorg. Chem. Front.*, 2017, **4**, 701-705. http://doi.org/10.1039/C6QI00543H.

44. Y. Rechkemmer, F. D. Breitgoff, M. van der Meer, M. Atanasov, M. Hakl, M. Orlita, P. Neugebauer, F. Neese, B. Sarkar and J. van Slageren, A Four-Coordinate Cobalt(II) Single-Ion Magnet with Coercivity and a Very High Energy Barrier. *Nat. Commun.*, 2016, **7**, 10467. http://doi.org/10.1038/ncomms10467.

View Article Online
DOI: 10.1039/D5NJ01857A

45. E. Carl, S. Demeshko, F. Meyer and D. Stalke, Triimidosulfonates as Acute Bite-Angle Chelates: Slow Relaxation of the Magnetization in Zero Field and Hysteresis Loop of a Co^{II} Complex. *Chem. Eur. J.*, 2015, **21**, 10109-10115. https://doi.org/10.1002/chem.201406083.

46. J. Vallejo, E. Pardo, M. Viciano-Chumillas, I. Castro, P. Amorós, M. Déniz, C. Ruiz-Pérez, C. Yuste-Vivas, J. Krzystek, M. Julve, F. Lloret and J. Cano, Reversible solvatomagnetic switching in a single-ion magnet from an entatic state. *Chem. Sci.*, 2017, **8**, 3694-3702. http://doi.org/10.1039/C6SC05188J.

47. R. Bruno, J. Vallejo, N. Marino, G. De Munno, J. Krzystek, J. Cano, E. Pardo and D. Armentano, Cytosine Nucleobase Ligand: A Suitable Choice for Modulating Magnetic Anisotropy in Tetrahedrally Coordinated Mononuclear Co^{II} Compounds. *Inorg. Chem.*, 2017, **56**, 1857-1864. https://doi.org/10.1021/acs.inorgchem.6b02448.

48. Y.-Y. Zhu, F. Liu, J.-J. Liu, Y.-S. Meng, S.-D. Jiang, A.-L. Barra, W. Wernsdorfer and S. Gao, Slow Magnetic Relaxation in Weak Easy-Plane Anisotropy: the Case of a Combined Magnetic and HFEPR Study. *Inorg. Chem.*, 2017, **56**, 697-700. https://doi.org/10.1021/acs.inorgchem.6b01972.

49. L. H. G. Kalinke, J. C. O. Cardoso, R. Rabelo, A. K. Valdo, F. T. Martins, J. Cano, M. Julve, F. Lloret and D. Cangussu, From Paramagnetic to Single-Molecule Magnet Behaviour in Heterobimetallic Compounds Containing the Tetrakis(thiocyanato-κN)cobaltate(II) Anion. *Eur. J. Inorg. Chem.*, 2018, **2018**, 816-825. https://doi.org/10.1002/ejic.201701177.

50. D. Shao, L.-D. Deng, L. Shi, D.-Q. Wu, X.-Q. Wei, S.-R. Yang and X.-Y. Wang, Slow Magnetic Relaxation and Spin-Crossover Behavior in a Bicomponent Ion-Pair Cobalt(II) Complex. *Eur. J. Inorg. Chem.*, 2017, **2017**, 3862-3867. https://doi.org/10.1002/ejic.201700719.

51. J. Palion-Gazda, B. Machura, R. Kruszynski, T. Grancha, N. Moliner, F. Lloret and M. Julve, Spin Crossover in Double Salts Containing Six- and Four-Coordinate Cobalt(II) Ions. *Inorg. Chem.*, 2017, **56**, 6281-6296. https://doi.org/10.1021/acs.inorgchem.7b00360.

52. , !!! INVALID CITATION !!! .

View Article Online
DOI: 10.1039/D5NJ01857A

53. J. Juráková, V. T. Santana, J. Pavlik, J. Moncoľ, I. Nemec, M. Clemente-León, S. K. Kuppusamy, M. Ruben, E. Čižmár and I. Šalitroš, Magnetic anisotropy and slow relaxation of magnetisation in double salts containing four- and six-coordinate cobalt(II) complex ions. *Dalton Trans.*, 2024, **53**, 12962-12972. http://doi.org/10.1039/D4DT01509F.

54. S.-Y. Chen, W. Lv, H.-H. Cui, L. Chen, Y.-Q. Zhang, X.-T. Chen, Z. Wang, Z.-W. Ouyang, H. Yan and Z.-L. Xue, Magnetic Anisotropies and Slow Magnetic Relaxation of Three Tetrahedral Tetrakis(pseudohalido)–Cobalt(II) Complexes. *New J. Chem.*, 2021, **45**, 16852-16861. http://doi.org/10.1039/D1NJ01916C.

55. A. Piecha-Bisiorek, A. Bieńko, R. Jakubas, R. Boča, M. Weselski, V. Kinzhybalo, A. Pietraszko, M. Wojciechowska, W. Medycki and D. Kruk, Physical and Structural Characterization of Imidazolium-Based Organic–Inorganic Hybrid: $(C_3N_2H_5)_2[CoCl_4]$. *J. Phys. Chem. A*, 2016, **120**, 2014-2021. https://doi.org/10.1021/acs.jpca.5b11924.

56. O. Y. Vassilyeva, E. A. Buvaylo, V. N. Kokozay, B. W. Skelton, C. Rajnák, J. Titiš and R. Boča, Long magnetic relaxation time of tetracoordinate Co^{2+} in imidazo[1,5-a]pyridinium-based $(C_{13}H_{12}N_3)_2[CoCl_4]$ hybrid salt and $[Co(C_{13}H_{12}N_3)Cl_3]$ molecular complex. *Dalton Trans.*, 2019, **48**, 11278-11284. http://doi.org/10.1039/C9DT01642B.

57. J. Martínez-Lillo, J. Faus, F. Lloret and M. Julve, Towards Multifunctional Magnetic Systems Through Molecular-Programmed Self Assembly of Re(IV) Metalloligands. *Coord. Chem. Rev.*, 2015, **289-290**, 215-237. https://doi.org/10.1016/j.ccr.2014.11.007.

58. C. Rojas-Dotti, A. Sanchis-Perucho, M. Orts-Arroyo, N. Moliner, R. Gonzalez, F. Lloret and J. Martinez-Lillo, Field-Induced Single-Ion Magnet Phenomenon in Hexabromo- and Hexaiodorhenate(IV) Complexes. *Magnetochemistry*, 2020, **6**, 20. https://doi.org/10.3390/magnetochemistry6020020.

59. J. Martínez-Lillo, T. F. Mastropietro, E. Lhotel, C. Paulsen, J. Cano, G. De Munno, J. Faus, F. Lloret, M. Julve, S. Nellutla and J. Krzystek, Highly Anisotropic Rhenium(IV) Complexes: New Examples of Mononuclear Single-Molecule Magnets. *J. Am. Chem. Soc.*, 2013, **135**, 13737-13748. https://doi.org/10.1021/ja403154z.

60. D. H. Moseley, S. E. Stavretis, K. Thirunavukkuarasu, M. Ozerov, Y. Cheng, L. L. Daemen, J. Ludwig, Z. Lu, D. Smirnov, C. M. Brown, A. Pandey, A. J. Ramirez-Cuesta, A. C. Lamb, M. Atanasov, E. Bill, F. Neese and Z.-L. Xue, Spin–phonon couplings in

View Article Online
DOI: 10.1039/D5NJ01857A

transition metal complexes with slow magnetic relaxation. *Nat. Comm.*, 2018, **9**, 2572. https://doi.org/10.1038/s41467-018-04896-0.

61. R. Sen and A. Mondal, Isolation of Octahedral to Tetrahedral Cobalt-Azido Molecular Assemblies Based on Cationic Influence. *J. Mol. Struct.*, 2019, **1198**, 126882. https://doi.org/10.1016/j.molstruc.2019.126882.
62. S. S. Massoud, M. Dubin, A. E. Guilbeau, M. Spell, R. Vicente, P. Wilfling, R. C. Fischer and F. A. Mautner, Azido- and thiocyanato-cobalt(II) complexes based pyrazole ligands. *Polyhedron*, 2014, **78**, 135-140. https://doi.org/10.1016/j.poly.2014.04.025.
63. J. R. Pilbrow, Effective *g* values for $S = 3/2$ and $S = 5/2$. *J. Magn. Reson.*, 1978, **31**, 479-490. https://doi.org/10.1016/S0022-2364(78)80015-8.
64. P. Gast and E. J. J. Groenen, EPR Interactions – *g*-Anisotropy. *eMagRes*, 2016, DOI: https://doi.org/10.1002/9780470034590.emrstm1500, 1435-1444. https://doi.org/10.1002/9780470034590.emrstm1500.
65. F. A. Cotton, *Chemical Applications of Group Theory*, Wiley, New York, 3 edn., 1990.
66. P. C. Bunting, M. Atanasov, E. Damgaard-Møller, M. Perfetti, I. Crassee, M. Orlita, J. Overgaard, J. van Slageren, F. Neese and J. R. Long, A linear cobalt(II) complex with maximal orbital angular momentum from a non-Aufbau ground state. *Science*, 2018, **362**, eaat7319. https://doi.org/10.1126/science.aat7319.
67. S. E. Stavretis, D. H. Moseley, F. Fei, H.-H. Cui, Y. Cheng, A. A. Podlesnyak, X. Wang, L. L. Daemen, C. M. Hoffmann, M. Ozerov, Z. Lu, K. Thirunavukkuarasu, D. Smirnov, T. Chang, Y.-S. Chen, A. J. Ramirez-Cuesta, X.-T. Chen and Z.-L. Xue, Spectroscopic Studies of the Magnetic Excitation and Spin-Phonon Couplings in a Single-Molecule Magnet. *Chem. Eur. J.*, 2019, **25**, 15846-15857. https://doi.org/10.1002/chem.201903635.
68. D. H. Moseley, Z. Liu, A. N. Bone, S. E. Stavretis, S. K. Singh, M. Atanasov, Z. Lu, M. Ozerov, K. Thirunavukkuarasu, Y. Cheng, L. L. Daemen, D. Lubert-Perquel, D. Smirnov, F. Neese, A. J. Ramirez-Cuesta, S. Hill, K. R. Dunbar and Z.-L. Xue, Comprehensive Studies of Magnetic Transitions and Spin–Phonon Couplings in the Tetrahedral Cobalt Complex $Co(AsPh_3)_2I_2$. *Inorg. Chem.*, 2022, **61**, 17123-17136. https://doi.org/10.1021/acs.inorgchem.2c02604.

View Article Online
DOI: 10.1039/D5NJ01857A

69. A. N. Bone, S. E. Stavretis, J. Krzystek, Z. Liu, Q. Chen, Z. Gai, X. Wang, C. A. Steren, X. B. Powers, A. A. Podlesnyak, X.-T. Chen, J. Telser, H. Zhou and Z.-L. Xue, Manganese tetraphenylporphyrin bromide and iodide. Studies of structures and magnetic properties. *Polyhedron*, 2020, **184**, 114488. https://doi.org/10.1016/j.poly.2020.114488.

70. P. Tin, S. E. Stavretis, M. Ozerov, J. Krzystek, A. N. Ponomaryov, S. A. Zvyagin, J. Wosnitza, C.-C. Chen, P. P. Y. Chen, J. Telser and Z.-L. Xue, Advanced Magnetic Resonance Studies of Tetraphenylporphyrinatoiron(III) Halides. *Appl. Magn. Reson.*, 2020, **51**, 1411-1432. https://doi.org/10.1007/s00723-020-01236-8.

71. M. Viciano-Chumillas, G. Blondin, M. Clémancey, J. Krzystek, M. Ozerov, D. Armentano, A. Schnegg, T. Lohmiller, J. Telser, F. Lloret and J. Cano, Single-Ion Magnetic Behaviour in an Iron(III) Porphyrin Complex: A Dichotomy Between High Spin and 5/2–3/2 Spin Admixture. *Chem. Eur. J.*, 2020, **26**, 14242-14251. https://doi.org/10.1002/chem.202003052.

72. K. D. Hughey, N. C. Harms, K. R. O'Neal, A. J. Clune, J. C. Monroe, A. L. Blockmon, C. P. Landee, Z. Liu, M. Ozerov and J. L. Musfeldt, Spin–Lattice Coupling Across the Magnetic Quantum-Phase Transition in Copper-Containing Coordination Polymers. *Inorg. Chem.*, 2020, **59**, 2127-2135. https://doi.org/10.1021/acs.inorgchem.9b02394.

73. J. Vallejo, M. Viciano-Chumillas, F. Lloret, M. Julve, I. Castro, J. Krzystek, M. Ozerov, D. Armentano, G. De Munno and J. Cano, Coligand Effects on the Field-Induced Double Slow Magnetic Relaxation in Six-Coordinate Cobalt(II) Single-Ion Magnets (SIMs) with Positive Magnetic Anisotropy. *Inorg. Chem.*, 2019, **58**, 15726-15740. https://doi.org/10.1021/acs.inorgchem.9b01719.

74. L. Devkota, D. J. SantaLucia, A. M. Wheaton, A. J. Pienkos, S. V. Lindeman, J. Krzystek, M. Ozerov, J. F. Berry, J. Telser and A. T. Fiedler, Spectroscopic and Magnetic Studies of Co(II) Scorpionate Complexes: Is There a Halide Effect on Magnetic Anisotropy? *Inorg. Chem.*, 2023, **62**, 5984-6002. https://doi.org/10.1021/acs.inorgchem.2c04468.

75. E. Ferentinos, D. Tzeli, S. Sottini, E. J. J. Groenen, M. Ozerov, G. Poneti, K. Kaniewska-Laskowska, J. Krzystek and P. Kyritsis, Magnetic anisotropy and structural flexibility in the field-induced single ion magnets [Co{$(OPPh_2)(EPPh_2)N$}$_2$], E = S, Se, explored by

View Article Online
DOI: 10.1039/D5NJ01857A

experimental and computational methods. *Dalton Trans.*, 2023, **52**, 2036-2050. http://doi.org/10.1039/D2DT03335F.

76. A. Landart-Gereka, M. M. Quesada-Moreno, M. A. Palacios, I. F. Díaz-Ortega, H. Nojiri, M. Ozerov, J. Krzystek and E. Colacio, Pushing up the easy-axis magnetic anisotropy and relaxation times in trigonal prismatic Co^{II} mononuclear SMMs by molecular structure design. *Chem. Commun.*, 2023, **59**, 952-955. http://doi.org/10.1039/D2CC06012D.

77. P. Kumar, D. J. SantaLucia, K. Kaniewska-Laskowska, S. V. Lindeman, A. Ozarowski, J. Krzystek, M. Ozerov, J. Telser, J. F. Berry and A. T. Fiedler, Probing the Magnetic Anisotropy of Co(II) Complexes Featuring Redox-Active Ligands. *Inorg. Chem.*, 2020, **59**, 16178-16193. https://doi.org/10.1021/acs.inorgchem.0c01812.

78. J. G. C. Kragskow, J. Marbey, C. D. Buch, J. Nehrkorn, M. Ozerov, S. Piligkos, S. Hill and N. F. Chilton, Analysis of vibronic coupling in a 4f molecular magnet with FIRMS. *Nat. Commun.*, 2022, **13**, 825. https://doi.org/10.1038/s41467-022-28352-2.

79. M. Perfetti, M. Gysler, Y. Rechkemmer-Patalen, P. Zhang, H. Taştan, F. Fischer, J. Netz, W. Frey, L. W. Zimmermann, T. Schleid, M. Hakl, M. Orlita, L. Ungur, L. Chibotaru, T. Brock-Nannestad, S. Piligkos and J. van Slageren, Determination of the electronic structure of a dinuclear dysprosium single molecule magnet without symmetry idealization. *Chem. Sci.*, 2019, **10**, 2101-2110. http://doi.org/10.1039/C8SC03170C.

80. C. N. Widener, A. N. Bone, M. Ozerov, R. Richardson, Z. Lu, K. Thirunavukkuarasu, D. Smirnov, X.-T. Chen and Z.-L. Xue, Direct Observation of Magnetic Transitions in a Nickel(II) Complex with Large Anisotropy. *Chin. J. Inorg. Chem.*, 2020, **35**, 1149-1156. http://doi.org/10.11862/CJIC.2020.126.

81. M. J. Jenkins, M. Ozerov, J. Krzystek, L. L. Daemen, Y. Cheng and Z.-L. Xue, Probing magnetic and vibrational properties of trigonal-bipyramidal Co(II) and Ni(II) complexes using advanced spectroscopies. *New J. Chem.*, 2025, **49**, 5740-5756. http://doi.org/10.1039/D5NJ00184F.

82. J. Krzystek, D. C. Swenson, S. A. Zvyagin, D. Smirnov, A. Ozarowski and J. Telser, Cobalt(II) "Scorpionate" Complexes as Models for Cobalt-Substituted Zinc Enzymes: Electronic Structure Investigation by High-Frequency and -Field Electron Paramagnetic Resonance Spectroscopy. *J. Am. Chem. Soc.*, 2010, **132**, 5241-5253. https://doi.org/10.1021/ja910766w.

View Article Online
DOI: 10.1039/D5NJ01857A

83. A. L. Nagelski, M. Ozerov, M. S. Fataftah, J. Krzystek, S. M. Greer, P. L. Holland and J. Telser, Electronic Structure of Three-Coordinate Fe^{II} and Co^{II} β-Diketiminate Complexes. *Inorg. Chem.*, 2024, **63**, 4511-4526. https://doi.org/10.1021/acs.inorgchem.3c03388.

84. A. Świtlicka, B. Machura, M. Penkala, A. Bieńko, D. C. Bieńko, J. Titiš, C. Rajnák, R. Boča, A. Ozarowski and M. Ozerov, Slow Magnetic Relaxation in Cobalt(II) Field-Induced Single-Ion Magnets with Positive Large Anisotropy. *Inorg. Chem.*, 2018, **57**, 12740-12755. https://doi.org/10.1021/acs.inorgchem.8b01906.

85. K. Choroba, J. Palion-Gazda, B. Machura, A. Bieńko, D. Wojtala, D. Bieńko, C. Rajnák, R. Boča, A. Ozarowski and M. Ozerov, Large Magnetic Anisotropy in Mono- and Binuclear Cobalt(II) Complexes: The Role of the Distortion of the Coordination Sphere in Validity of the Spin-Hamiltonian Formalism. *Inorg. Chem.*, 2024, **63**, 1068-1082. https://doi.org/10.1021/acs.inorgchem.3c03405.

86. W. Lv, L. Chen, X.-T. Chen, H. Yan, Z. Wang, Z.-W. Ouyang and Z.-L. Xue, Structures and magnetic anisotropies of two seven-coordinate Co(II)–nitrate complexes showing slow magnetic relaxation. *New J. Chem.*, 2023, **47**, 15553-15560. http://doi.org/10.1039/D3NJ02160B.

87. H.-H. Cui, Y.-Q. Zhang, X.-T. Chen, Z. Wang and Z.-L. Xue, Magnetic anisotropy and slow magnetic relaxation processes of cobalt(II)-pseudohalide complexes. *Dalton Trans.*, 2019, **48**, 10743-10752. http://doi.org/10.1039/C9DT00644C.

88. S.-Y. Chen, H.-H. Cui, Y.-Q. Zhang, Z. Wang, Z.-W. Ouyang, L. Chen, X.-T. Chen, H. Yan and Z.-L. Xue, Magnetic anisotropy and relaxation behavior of six-coordinate tris(pivalato)-Co(II) and -Ni(II) complexes. *Dalton Trans.*, 2018, **47**, 10162-10171. http://doi.org/10.1039/C8DT01554F.

89. W. Lv, H.-H. Cui, L. Chen, Y.-Q. Zhang, X.-T. Chen, Z. Wang, Z.-W. Ouyang and Z.-L. Xue, Magnetic anisotropy of two tetrahedral Co(II)-halide complexes with triphenylphosphine ligands. *Dalton Trans.*, 2022, **51**, 7530-7538. http://doi.org/10.1039/D2DT00121G.

90. H.-H. Cui, M.-M. Ding, X.-D. Zhang, W. Lv, Y.-Q. Zhang, X.-T. Chen, Z. Wang, Z.-W. Ouyang and Z.-L. Xue, Magnetic anisotropy in square pyramidal cobalt(II) complexes

View Article Online
DOI: 10.1039/D5NJ01857A

supported by a tetraazo macrocyclic ligand. *Dalton Trans.*, 2020, **49**, 14837-14846. http://doi.org/10.1039/D0DT01954B.

91. J. Krzystek, A. Ozarowski and J. Telser, Multi-frequency, high-field EPR as a powerful tool to accurately determine zero-field splitting in high-spin transition metal coordination complexes. *Coord. Chem. Rev.*, 2006, **250**, 2308-2324. https://doi.org/10.1016/j.ccr.2006.03.016.

92. T. Dubroca, A. Ozarowski, Y. Sunatsuki, J. Telser, S. Hill and J. Krzystek, Benefitting from Magnetic Field-Induced Torquing in Terahertz EPR of a Mn^{III} Coordination Complex. *Appl. Magn. Reson.*, 2025, **56**, 137-149. https://doi.org/10.1007/s00723-024-01706-3.

93. P. Baltzer, A. Furrer, J. Hulliger and A. Stebler, Magnetic properties of nickelocene. A reinvestigation using inelastic neutron scattering and magnetic susceptibility. *Inorg. Chem.*, 1988, **27**, 1543-1548. https://doi.org/10.1021/ic00282a007.

94. G. Amoretti, R. Caciuffo, S. Carretta, T. Guidi, N. Magnani and P. Santini, Inelastic neutron scattering investigations of molecular nanomagnets. *Inorg. Chim. Acta.*, 2008, **361**, 3771-3776. https://doi.org/10.1016/j.ica.2008.03.047.

95. P. C. H. Mitchell, S. F. Parker, A. J. Ramirez-Cuesta and J. Tomkinson, *Vibrational Spectroscopy with Neutrons: With Applications in Chemistry, Biology, Materials Science and Catalysis*, World Scientific Publishing Company, 2005. https://www.worldscientific.com/worldscibooks/10.1142/5628.

96. M. A. Dunstan, R. A. Mole and C. Boskovic, Inelastic Neutron Scattering of Lanthanoid Complexes and Single-Molecule Magnets. *Eur. J. Inorg. Chem.*, 2019, **2019**, 1090-1105. https://doi.org/10.1002/ejic.201801306.

97. E. J. L. McInnes, Spectroscopy of Single-Molecule Magnets. *Struct. Bond. (Single-Molecule Magnets and Related Phenomena)*, 2006, DOI: 10.1007/430_034, 69-102. https://doi.org/10.1007/430_034.

98. E. Colacio, J. Ruiz, E. Ruiz, E. Cremades, J. Krzystek, S. Carretta, J. Cano, T. Guidi, W. Wernsdorfer and E. K. Brechin, Slow Magnetic Relaxation in a Co^{II}–Y^{III} Single-Ion Magnet with Positive Axial Zero-Field Splitting. *Angew. Chem. In. Ed.*, 2013, **52**, 9130-9134. https://doi.org/10.1002/anie.201304386.

View Article Online
DOI: 10.1039/D5NJ01857A

99. K. S. Pedersen, L. Ungur, M. Sigrist, A. Sundt, M. Schau-Magnussen, V. Vieru, H. Mutka, S. Rols, H. Weihe, O. Waldmann, L. F. Chibotaru, J. Bendix and J. Dreiser, Modifying the Properties of 4f Single-Ion Magnets by Peripheral Ligand Functionalisation. *Chem. Sci.*, 2014, **5**, 1650-1660. http://doi.org/10.1039/C3SC53044B.

100. X. Feng, J.-L. Liu, K. S. Pedersen, J. Nehrkorn, A. Schnegg, K. Holldack, J. Bendix, M. Sigrist, H. Mutka, D. Samohvalov, D. Aguilà, M.-L. Tong, J. R. Long and R. Clérac, Multifaceted magnetization dynamics in the mononuclear complex $[Re^{IV}Cl_4(CN)_2]^{2-}$. *Chem. Commun.*, 2016, **52**, 12905-12908. http://doi.org/10.1039/C6CC05473K.

101. M. A. Sørensen, U. B. Hansen, M. Perfetti, K. S. Pedersen, E. Bartolomé, G. G. Simeoni, H. Mutka, S. Rols, M. Jeong, I. Zivkovic, M. Retuerto, A. Arauzo, J. Bartolomé, S. Piligkos, H. Weihe, L. H. Doerrer, J. van Slageren, H. M. Rønnow, K. Lefmann and J. Bendix, Chemical tunnel-splitting-engineering in a dysprosium-based molecular nanomagnet. *Nat. Commun.*, 2018, **9**, 1292. https://doi.org/10.1038/s41467-018-03706-x.

102. M. Perfetti, M. A. Sørensen, U. B. Hansen, H. Bamberger, S. Lenz, P. P. Hallmen, T. Fennell, G. G. Simeoni, A. Arauzo, J. Bartolomé, E. Bartolomé, K. Lefmann, H. Weihe, J. van Slageren and J. Bendix, Magnetic Anisotropy Switch: Easy Axis to Easy Plane Conversion and Vice Versa. *Adv. Funct. Mater.*, 2018, **28**, 1801846. https://doi.org/10.1002/adfm.201801846.

103. M. Vonci, M. J. Giansiracusa, W. Van den Heuvel, R. W. Gable, B. Moubaraki, K. S. Murray, D. Yu, R. A. Mole, A. Soncini and C. Boskovic, Magnetic Excitations in Polyoxotungstate-Supported Lanthanoid Single-Molecule Magnets: An Inelastic Neutron Scattering and ab Initio Study. *Inorg. Chem.*, 2017, **56**, 378-394. https://doi.org/10.1021/acs.inorgchem.6b02312.

104. M. Vonci, M. J. Giansiracusa, R. W. Gable, W. Van den Heuvel, K. Latham, B. Moubaraki, K. S. Murray, D. Yu, R. A. Mole, A. Soncini and C. Boskovic, Ab initio calculations as a quantitative tool in the inelastic neutron scattering study of a single-molecule magnet analogue. *Chem. Commun.*, 2016, **52**, 2091-2094. http://doi.org/10.1039/C5CC07541F.

105. N. A. Bonde, J. B. Petersen, M. A. Sørensen, U. G. Nielsen, B. Fåk, S. Rols, J. Ollivier, H. Weihe, J. Bendix and M. Perfetti, Importance of Axial Symmetry in Elucidating

View Article Online
DOI: 10.1039/D5NJ01857A

Lanthanide–Transition Metal Interactions. *Inorg. Chem.*, 2020, **59**, 235-243. https://doi.org/10.1021/acs.inorgchem.9b02064.

106. S. C. Hunter, A. A. Podlesnyak and Z.-L. Xue, Magnetic Excitations in Metalloporphyrins by Inelastic Neutron Scattering: Determination of Zero-Field Splittings in Iron, Manganese, and Chromium Complexes. *Inorg. Chem.*, 2014, **53**, 1955-1961. https://doi.org/10.1021/ic4028354.

107. S. E. Stavretis, M. Atanasov, A. A. Podlesnyak, S. C. Hunter, F. Neese and Z.-L. Xue, Magnetic Transitions in Iron Porphyrin Halides by Inelastic Neutron Scattering and Ab Initio Studies of Zero-Field Splittings. *Inorg. Chem.*, 2015, **54**, 9790-9801. https://doi.org/10.1021/acs.inorgchem.5b01505.

108. Z.-L. Xue, A. J. Ramirez-Cuesta, C. M. Brown, S. Calder, H. Cao, B. C. Chakoumakos, L. L. Daemen, A. Huq, A. I. Kolesnikov, E. Mamontov, A. A. Podlesnyak and X. Wang, Neutron Instruments for Research in Coordination Chemistry. *Eur. J. Inorg. Chem.*, 2019, 1065-1089. https://doi.org/10.1002/ejic.201801076.

109. J. Krzystek and J. Telser, Measuring giant anisotropy in paramagnetic transition metal complexes with relevance to single-ion magnetism. *Dalton Trans.*, 2016, **45**, 16751-16763. http://doi.org/10.1039/C6DT01754A.

110. A. T. Hand, B. D. Watson-Sanders and Z.-L. Xue, Spectroscopic techniques to probe magnetic anisotropy and spin–phonon coupling in metal complexes. *Dalton Trans.*, 2024, **53**, 4390-4405. http://doi.org/10.1039/D3DT03609J.

111. G. C. Brackett, P. L. Richards and W. S. Caughey, Far-Infrared Magnetic Resonance in Fe(III) and Mn(III) Porphyrins, Myoglobin, Hemoglobin, Ferrichrome A, and Fe(III) Dithiocarbamates. *J. Chem. Phys.*, 1971, **54**, 4383-4401. https://doi.org/10.1063/1.1674688.

112. G. C. Brackett, Far-Infrared Magnetic Resonance in Fe(III) and Mn(III) Porphyrins, Myoglobin, Hemoglobin, Ferrichrome A, and Fe(III) Dithiocarbamates. Ph.D. dissertation, University of California, Berkeley, 1970.

113. D. H. Moseley, S. E. Stavretis, K. Thirunavukkuarasu, M. Ozerov, Y. Cheng, L. L. Daemen, J. Ludwig, Z. Lu, D. Smirnov, C. M. Brown, A. Pandey, A. J. Ramirez-Cuesta, A. C. Lamb, M. Atanasov, E. Bill, F. Neese and Z.-L. Xue, Spin–phonon couplings in

View Article Online
DOI: 10.1039/D5NJ01857A

transition metal complexes with slow magnetic relaxation. *Nat. Commun.*, 2018, **9**, 2572. https://doi.org/10.1038/s41467-018-04896-0.

114. D. H. Moseley, S. E. Stavretis, Z. Zhu, M. Guo, C. M. Brown, M. Ozerov, Y. Cheng, L. L. Daemen, R. Richardson, G. Knight, K. Thirunavukkuarasu, A. J. Ramirez-Cuesta, J. Tang and Z.-L. Xue, Inter-Kramers Transitions and Spin–Phonon Couplings in a Lanthanide-Based Single-Molecule Magnet. *Inorg. Chem.*, 2020, **59**, 5218-5230. https://doi.org/10.1021/acs.inorgchem.0c00523.

115. J. Krzystek, S. A. Zvyagin, A. Ozarowski, S. Trofimenko and J. Telser, Tunable-Frequency High-Field Electron Paramagnetic Resonance. *Journal of Magnetic Resonance*, 2006, **178**, 174-183. https://doi.org/10.1016/j.jmr.2005.09.007.

116. S. Stoll and A. Schweiger, EasySpin, a comprehensive software package for spectral simulation and analysis in EPR. *J. Magn. Reson.*, 2006, **178**, 42-55. https://doi.org/10.1016/j.jmr.2005.08.013.

117. R. Boča, J. Titiš, C. Rajnák and J. Krzystek, Positive zero-field splitting and unexpected slow magnetic relaxation in the magneto-chemical calibrant $HgCo(NCS)_4$. *Dalton Trans.*, 2021, **50**, 3468-3472. http://doi.org/10.1039/D1DT00407G.

118. D. Maganas, J. Krzystek, E. Ferentinos, A. M. Whyte, N. Robertson, V. Psycharis, A. Terzis, F. Neese and P. Kyritsis, Investigating Magnetostructural Correlations in the Pseudooctahedral trans-$[Ni^{II}\{(OPPh_2)(EPPh_2)N\}_2(sol)_2]$ Complexes (E = S, Se; sol = DMF, THF) by Magnetometry, HFEPR, and ab Initio Quantum Chemistry. *Inorg. Chem.*, 2012, **51**, 7218-7231. https://doi.org/10.1021/ic300453y.

119. R. J. Ortiz, M. Shepit, J. van Lierop, J. Krzystek, J. Telser and D. E. Herbert, Characterization of the Ligand Field in Pseudo-Octahedral Ni(II) Complexes of Pincer-Type Amido Ligands: Magnetism, Redox Behavior, Electronic Absorption and High-Frequency and -Field EPR Spectroscopy. *Eur. J. Inorg. Chem.*, 2023, **26**, e202300446. https://doi.org/10.1002/ejic.202300446.

120. L. Chen, H.-H. Cui, S. E. Stavretis, S. C. Hunter, Y.-Q. Zhang, X.-T. Chen, Y.-C. Sun, Z. Wang, Y. Song, A. A. Podlesnyak, Z.-W. Ouyang and Z.-L. Xue, Slow Magnetic Relaxations in Cobalt(II) Tetranitrate Complexes. Studies of Magnetic Anisotropy by Inelastic Neutron Scattering and High-Frequency and High-Field EPR Spectroscopy. *Inorg. Chem.*, 2016, **55**, 12603-12617. https://doi.org/10.1021/acs.inorgchem.6b01544.

View Article Online
DOI: 10.1039/D5NJ01857A

121. Z.-B. Hu, L.-A. Gui, L.-H. Li, T.-T. Xiao, A. T. Hand, P. Tin, M. Ozerov, Y. Peng, Z. Ouyang, Z. Wang, Z.-L. Xue and Y. Song, Co^{II} single-ion magnet and its multi-dimensional aggregations: Influence of the structural rigidity on magnetic relaxation process. *Chin. Chem. Lett.*, 2025, **36**, 109600. https://doi.org/10.1016/j.cclet.2024.109600.

122. P. Alemany, D. Casanova, S. Alvarez, C. Dryzun and D. Avnir, Continuous Symmetry Measures: A New Tool in Quantum Chemistry. *Rev. Comput. Chem.*, 2017, **30**, 289-352. https://doi.org/10.1002/9781119356059.ch7.

123. T. Schönherr, M. Atanasov and H. Adamsky, *Angular Overlap Model*, in *Comprehensive Coordination Chemistry II*, eds. J. A. McCleverty and T. J. Meyer, Pergamon, 2003, pp. 443-455. https://doi.org/10.1016/B0-08-043748-6/01052-5.

124. C. E. Schäffer, A perturbation representation of weak covalent bonding. *Struct. Bonding*, 1968, **5**, 68-95. https://doi.org/10.1007/BFb0118847.

125. G. L. Miessler, P. J. Fischer and D. A. Tarr, *Inorganic Chemistry, 5th ed.*, 2014.

126. A. J. Bridgeman and M. Gerloch, The Interpretation of Ligand Field Parameters. *Prog. Inorg. Chem.*, 1997, **45**, 179-281.

127. J. Telser, The DDN software is available at https://edmond.mpg.de/dataset.xhtml?persistentId=doi:10.17617/3.XNQCUE, labeled as "Josh_Telser_sfotware.zip".).

128. J. Bendix, *Ligfield*, in *Comprehensive Coordination Chemistry II*, eds. J. A. McCleverty and T. J. Meyer, 2003, pp. 673-676. https://doi.org/10.1016/B0-08-043748-6/01118-X.

129. J. C. Slater, *Quantum Theory of Atomic Structure*, McGraw-Hill, 1960.

130. P. Senise, On the Reaction between Cobalt(II) and Azide Ions in Aqueous and Aqueous-organic Solutions. *J. Am. Chem. Soc.*, 1959, **81**, 4196-4199. https://doi.org/10.1021/ja01525a020.

131. A. K. Hassan, L. A. Pardi, J. Krzystek, A. Sienkiewicz, P. Goy, M. Rohrer and L. C. Brunel, Ultrawide Band Multifrequency High-Field EMR Technique: A Methodology for Increasing Spectroscopic Information. *J. Magn. Reson.*, 2000, **142**, 300-312. https://doi.org/10.1006/jmre.1999.1952.

132. B. A. Dougan and Z. Xue, Polarized neutron diffraction and its application to spin density studies. *Sci. China B*, 2009, **52**, 2083. https://doi.org/10.1007/s11426-009-0199-4.

View Article Online
DOI: 10.1039/D5NJ01857A

133. A. Furrer, J. Mesot and T. Strässle, *Neutron Scattering in Condensed Matter Physics, p. 7*, World Scientific Publishing Company, 2009. https://www.worldscientific.com/worldscibooks/10.1142/4870.

134. R. Basler, C. Boskovic, G. Chaboussant, H. U. Güdel, M. Murrie, S. T. Ochsenbein and A. Sieber, Molecular Spin Clusters: New Synthetic Approaches and Neutron Scattering Studies. *ChemPhysChem*, 2003, **4**, 910-926. https://doi.org/10.1002/cphc.200300689.

135. G. A. Bain and J. F. Berry, Diamagnetic Corrections and Pascal's Constants. *J. Chem. Educ.*, 2008, **85**, 532. https://doi.org/10.1021/ed085p532.

View Article Online
DOI: 10.1039/D5NJ01857A

Data availability

Data are available from the authors upon request. The authors confirm that the data supporting the findings of this study are available within the article and its ESI.